The Influence of Oxychlorine Phases on the Flash Pyrolysis of Polycyclic Aromatic Hydrocarbons and Implications for Mars

Maeva Millan, Cyril Szopa, A Buch, P R Mahaffy, S S Johnson

Journal of Analytical and Applied Pyrolysis 181 (2024) 106578

Contents lists available at ScienceDirect

Journal of Analytical and Applied Pyrolysis

journal homepage: www.elsevier.com/locate/jaap

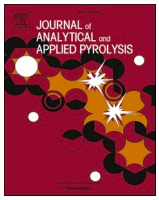

The influence of oxychlorine phases on the flash pyrolysis of polycyclic aromatic hydrocarbons and implications for mars

M. Millan [a,b,*], C. Szopa [a], A. Buch [c], P.R. Mahaffy [d], S.S. Johnson [b]

[a] Laboratoire Atmosphères, Observations Spatiales (LATMOS), LATMOS/IPSL, CNRS, UVSQ Université Paris-Saclay, Sorbonne Université, Guyancourt, France
[b] Department of Biology, Georgetown University, Washington, DC 20057, USA
[c] Laboratoire de Génie des Procédés et Matériaux (LGPM), Gif-sur-Yvette, France
[d] NASA Goddard Space Flight Center, Planetary Environments Laboratory, Greenbelt, MD 20771, USA

ARTICLE INFO

Keywords:
Chlorohydrocarbons
Oxychlorine phases
Polycyclic Aromatic Hydrocarbons (PAHs)
Flash pyrolysis
Gas chromatography mass spectrometry

ABSTRACT

A variety of chlorine-bearing hydrocarbons have been detected in the chemical analyses of soil and rock samples performed on Mars with the GCMS instruments onboard the Viking landers and the SAM instrument suite onboard the *Curiosity* rover. These aromatic and aliphatic chlorohydrocarbons are most likely produced by chemical reactions between salts (e.g., perchlorates, chlorates) and organic molecules of martian origin either during the thermal processing of the samples in flight or generated through radiation processes happening in Mars' near surface. To understand the influence of salts on the organic molecules during pyrolysis and identify the potential precursors of the chlorohydrocarbons detected on Mars, we performed a systematic study and pyrolyzed three polycyclic aromatic hydrocarbons (PAHs)—naphthalene, phenanthrene, and benzanthracene—in the presence of six perchlorate and chlorate salts that have been identified or are most likely present on Mars—calcium perchlorate, iron perchlorate, sodium perchlorate, magnesium perchlorate, sodium chlorate, and potassium chlorate. Iron perchlorate had the strongest (oxy)chlorination power on the PAHs of all the salts tested whereas magnesium perchlorate and potassium chlorate were the most destructive ones. Despite the presence of these caustic salts, PAHs were highly chemically and thermally stable, suggesting they would likely be detectable natively if present in a martian sample. In addition, chlorohydrocarbons that are characteristic of the parent PAH were formed and could be used to help identify the nature of a PAH. This investigation underlines that PAHs could be the precursors of aromatic chlorohydrocarbons detected on Mars, but a definitive identification will require the detection of the parent PAHs and their respective pyrolyzates, molecules that were not yet detected on Mars likely because of the flight operating constraints of the SAM instrument.

1. Introduction

Chloromethane and dichloromethane were the first chlorohydrocarbons detected on Mars by pyrolysis-gas chromatography/mass spectrometry (pyr-GC/MS) onboard the Viking landers in the 1970's. However, their origin was promptly attributed to terrestrial contamination [1,2]. Decades later, magnesium perchlorate was detected in terrains at a high northern latitude with the Wet Chemistry Laboratory onboard the Phoenix lander [3]. A few years later, the Sample Analysis at Mars (SAM) instrument onboard the *Curiosity* rover later confirmed these results and highlighted the presence of several oxychlorine phases including a variety of perchlorate, chlorate and chloride salts [4,5]. Following these results, the chorine-bearing organics detected by Viking were re-interpreted as possibly being produced from chemical reactions between the gases released from perchlorate salts and traces of organics present in the analyzed martian samples during the thermal processing of the samples at high temperature (> 200°C) to extract volatile materials [6]. The re-analysis of the Viking results has allowed the identification of chlorobenzene, likely produced from similar chemical reactions between martian organics and the oxychlorine phases present in the soil [7]. Since the landing of the *Curiosity* rover in 2012, the SAM results have extended the variety of organo-chlorinated compounds and salts detected to include new aliphatic chlorohydrocarbons, aromatic chlorohydrocarbons, as well as organic salts including oxalates and acetates [8–10]. Most of the aliphatic chlorohydrocarbons detected (e.g., chloroalkanes) were likely produced from reactions between the gases

* Correspondence to: 11 Boulevard d'Alembert, Guyancourt 78280, France.
E-mail address: maeva.millan@latmos.ipsl.fr (M. Millan).

https://doi.org/10.1016/j.jaap.2024.106578
Received 22 September 2023; Received in revised form 27 April 2024; Accepted 3 June 2024
Available online 14 June 2024

released from the salts and terrestrial organics present in the SAM Sample Manipulation System (SMS). However, the aromatic chlorohydrocarbons—including chlorobenzene and dichlorobenzene isomers—as well as dichloromethylpropane were likely produced from chemical reactions between the salts and the organic molecules present in the martian rock samples (mainly mudstones) collected by the rover [9,10]. Those indigenous chlorohydrocarbons could also be formed in Mars' near surface through direct UV, high energy X and y-rays radiations or low secondary X-ray radiations [11]. However, the nature and origin of these organic molecules indigenous to the samples still have to be determined. Laboratory studies have allowed to constrain some possible precursors of the chlorohydrocarbons detected with the SAM instrument [12], but the reactivity between organic molecules and oxychlorine phases remains poorly understood and undocumented. In order to further constrain the precursors of the chlorohydrocarbons, we conducted a systematic laboratory investigation to determine the influence of six oxychlorine phases that have been detected or are most likely present on Mars [13]—calcium perchlorate, iron perchlorate, sodium perchlorate, magnesium perchlorate, sodium chlorate, and potassium chlorate—during the flash pyrolysis of three PAHs—naphthalene, phenanthrene, and benzanthracene. PAHs and more specifically naphthalene, methyl-naphthalene, and dihydronaphthalene have been tentatively identified by the SAM instrument [14,15] and future analyses will be required to unambiguously confirm their origin(s). Other compounds likely coming from the decomposition of kerogen-like material have also been confirmed by the SAM instrument [14,16]. In addition, preliminary fluorescence measurements from the Scanning Habitable Environments with Raman and Luminescence of Organics and Chemicals (SHERLOC) instrument onboard *Perseverance,* the latest martian rover, have shown potential signatures of one- to two-ring aromatic compounds in various rocks present in Jezero crater, which may be related to the presence of PAHs [17].

The goals of this study were to (1) characterize the effects of the salts on the degradation or evolution of the PAHs and their decomposition products (*i.e.*, pyrolyzates) and their implications for the detection of PAHs on Mars, (2) constrain the nature of the salts and of the possible precursors of the chlorohydrocarbons detected on Mars, and (3) build a database of chlorohydrocarbons that could be present and searched in the Mars' *in situ* data. To do so, we first characterized the thermal behavior of the salts pure and mixed in a fused silica matrix using evolved gas analyses-mass spectrometry (EGA-MS) in order to aid interpret the pyr-GC/MS data. We then flash-pyrolysed the PAHs pure and mixed in fused silica matrix to evaluate its potential influence, and then with and without the six salts. One selected organic molecule−−naphthalene−was flash-pyrolyzed in the presence of Ca and Fe perchlorates both prepared in two different concentrations to assess the effect of concentration.

2. Material and methods

2.1. Samples

2.1.1. Oxychlorine phases

The temperature release of dioxygen observed in the SAM Evolved Gas Analyses (EGA) data ranged from 100 to 600°C. The highest temperatures were correlated with the thermal decomposition of Mg perchlorate, Na perchlorate, and Ca perchlorate whereas the lowest temperature range (100–200°C) correlated with Fe perchlorates/chlorates [18]. The intermediate temperatures may correspond to a mix of these minerals and/or to the presence of catalyzer minerals. For example, the presence of iron mineral phases (*e.g.*, hematite) can shift the release temperatures of the species and explain the variabilities observed in the different regions of Gale crater [18,19]. The spectroscopic analyses performed in the gullies have confirmed the presence of Mg perchlorate, Ca perchlorate, and Na perchlorate [20]. The abundance of ClO_4^- was estimated by the dioxygen release observed in the Rocknest (RN) sample to be between 0.3 and 0.5 wt% [21,22] and up to 1.3 wt% in the Cumberland (CB) sample [23]. The isotopic and ionic chromatography analyses performed on the martian meteorite EETA79001 highlighted the presence of ClO_4^- and ClO_3^- without identifying the nature of the counter ion [24].

Although the presence of the chlorate anion ClO_3^- was previously suggested [5], it was formally detected in martian Recurring Slope Lineae (RSL) in the form of Mg chlorate [20]. Laboratory experiments involving Mg chlorate were conducted in an attempt to match the release temperature of the various species detected in the SAM EGA data and new oxychlorine phases have been suggested, included chlorates [25]. In addition to Fe perchlorate, the release of O_2 at low temperatures is consistent with the thermal decomposition of chlorates [18,26]. The best candidate was suggested to be Ca chlorate, with O_2 and HCl release temperatures consistent with the release temperature observed in several samples analyzed with SAM [18]. However, this specific chlorate alone does not explain the release temperature of all the samples analyzed by SAM. The presence of other chlorates was thus suggested, including Mg chlorate, K chlorate, and Na chlorate [13,19]. When these chlorates are mixed with iron mineral phases (e.g., hematite, ferrihydrite, magnetite), the temperatures of release of O_2 and HCl match the ones measured with SAM.

Because of the variability in the nature of the salts likely present at the surface of Mars, six oxychlorine phases were chosen among the best candidates according to their dioxygen release temperature. These included four perchlorates—calcium perchlorate $Ca(ClO_4)_2$, iron perchlorate $Fe(ClO_4)_2$, sodium perchlorate $Na(ClO_4)_2$ and magnesium perchlorate $Mg(ClO_4)_2$—and two chlorates—sodium chlorate $Na(ClO_3)$ and potassium chlorate $K(ClO_3)$. All the salts were supplied by Sigma-Aldrich.

2.1.2. Polycyclic aromatic hydrocarbons (PAHs)

PAHs have been detected in the interstellar medium and on various objects in the solar system [27]. They are abundant in carbonaceous chondrites (CC) at concentrations varying between 15 and 3319 $\mu g.g^{-1}$ [28–30] and they can represent up to 80 % of the soluble organic matter [31]. The Insoluble Organic Matter is constituted of PAHs including up to 5–6 aromatic rings and they represent 70 wt% of the organic molecules present in meteorites [32]. PAHs are also abundant in micrometeorites and Interplanetary Dust Particles [33,34]. Therefore, they could have been brought to the Mars surface by these exogenous sources or synthetized indigenously on Mars during the maturation of organic matter from a biotic and/or abiotic origin, similarly to terrestrial PAHs [35]. They were also detected in 11 martian meteorites and could have been synthetized during the crystallization of the martian magma, and are thus likely present in martian basalts [36].

Among the PAHs detected in exogenous sources, we selected naphthalene ($C_{10}H_8$), phenanthrene ($C_{14}H_{10}$), and benzanthracene ($C_{18}H_{12}$) for this study because of their abundance in CC [30] and micrometeorites [37]. These PAHs, all supplied by Sigma-Aldrich, are constituted of 2–4 aromatic rings, allowing to consider the size of the molecule as a parameter in our investigation (Table 1).

2.2. Sample preparation

The six oxychlorine phases and three PAHs were prepared following the steps described in [12]. In short, fused silica, chosen for its presence on Mars [38,39] and presumed chemical inertia [40], was used as a solid matrix to "dilute" molecules and salts. Prior to dilution, the fused silica was conditioned at 900°C using a muffle furnace and potential contamination was assessed by pyr-GC/MS. Salts and PAHs were manually crushed and individually mixed in concentrations of 2 and 1 wt% respectively in silica. They were then mechanically mixed together by crushing 5 mg of each organic and oxychlorine and 10 mg of the final mixture oxychlorine-organics (2:1) was vortexed and weighted into a stainless-steel Eco-cup (FrontierLab) for pyrolysis. To confirm the

Table 1
Structures and physical properties of the PAHs selected for this study.

Compound	Raw chemical formula	Representation	Molar mass (g.mol^{-1})	Boiling point (°C)	Purity (%)
Napthalene	$C_{10}H_8$	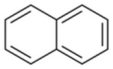	128.17	218	99
Phenanthrene	$C_{14}H_{10}$	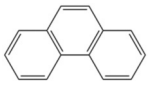	178.23	336	98
Benzanthracene	$C_{18}H_{12}$	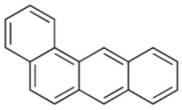	228.28	438	99

chemical inertia of the silica matrix on the species in our analytical conditions, we pyrolyzed 0.2–0.5 mg of each oxychlorine and PAH pure and mixed in fused silica and compared the results obtained (see sections III.1 and III.2).

2.3. Analytical method

The EGA-MS and pyr-GC/MS experiments were performed using a Frontier Laboratories 3030D multi-shot pyrolyzer (FrontierLab) directly mounted on the injector of a Trace 1300 gas chromatograph coupled to an ISQ mass spectrometer (ThermoFisher). For the EGA-MS experiments, the samples were pyrolyzed in SAM-like conditions from 80 to 850°C at 35°C min^{-1} and for the pyr-GC/MS experiments, the samples were flash-pyrolyzed at 850°C for 1 minute, which represents the maximum temperature that the SAM instrument can reach. This temperature and flash heating mode were chosen deliberately to induce the worst-case scenario reactions that could happen within the SAM instrument at high temperature and identify the subsequent reaction products.

The EGA-MS experiments were performed using a short inert metallic column (2.5 m long, 0.15 mm i.d.) which allows a rapid transfer of the volatiles to the MS and to establish the correlation between the time of analysis and the pyrolysis temperature. The GCMS experiments were performed using a Restek Rxi-5Sil MS column (30 m, 0.25 mm i.d., and 0.25 µm stationary phase thickness) including a 5 m deactivated long integra-guard tube. This general column, similar to those used on SAM, allows a good separation of C_5-C_{15} molecules while the guard column significantly reduced the production of byproducts from reactions between the salts and the phenyl compounds constituting the stationary phase of the GC column [41]. The carrier gas was helium (purity > 99.9999 %, Air Liquide) used with a column flow rate of 1 ml min^{-1} and a 1:10 split ratio. The GC column was heated from 33°C (held for 3 minutes) up to 300°C (held 1 minute) at a 6°C min^{-1} then 10°C min^{-1} rate. Ions were scanned in the *m/z* range 10–535 as in the SAM instrument. The temperatures of the interface of the pyrolyzer and of the injector were both set at 250°C whereas the transfer line and ion source were set at 350°C.

The EGA-MS of the salts were processed by highlighting the characteristic fragments of the species that could have an influence on the organic molecules, including water (H_2O: *m/z* 18), dioxygen (O_2: *m/z* 32), hydrochloric acid (HCl: *m/z* 36), and chlorine (Cl_2: *m/z* 70).

Control blanks with and without silica as well as silica with perchlorates only were performed before and between each sample analysis to assess potential contamination, the formation of byproducts due to the presence of salts as well as limit carry-over between each analysis. Peaks present in the total ion current (TIC) or in the extracted ion chromatograms (EIC) were identified using the Xcalibur software package (Thermofisher) and compared to the National Standard Institute of Technology (NIST) mass spectra database. Elution times of chemical standards were used to confirm the identifications of certain compounds.

Replicates of both the EGA-MS and the pyr-GC/MS experiments were performed to control the homogeneity of the samples. The qualitative results were similar and quantitative results were within the same order of magnitude which was sufficient for this study.

3. Results and discussion

3.1. EGA-MS of oxychlorines pure and in silica

Previous studies have shown that fused silica, supposedly chemically and thermally inert, can slightly influence the thermal behavior of Ca perchlorate [12]. As a comparison and to complete previous studies, the influence of silica was evaluated for the five other oxychlorine phases (pure and mixed at 10 wt% in silica) selected for this study. The analysis was focused on the nature and temperature of the species released, and the relative intensity of the peaks. The thermograms of the gases released by the oxychlorine phases during EGA are presented in Fig. 1.

Differences and similarities were observed regarding the nature, temperature, and relative abundance of the species released whether the salts were pyrolyzed in a pure form or in silica. The species released within the first hundred degrees, with the exception of water, were not considered because they are not associated to any known reaction (these are likely free species entering the helium path when the cup is dropped into the pyrolysis oven). Between 90 and 200°C, water is released for each (per)chlorate and is likely related to free water desorbing from the (per)chlorates and the silica, despite the precautions taken to avoid water adsorption (silica permanently kept on a heating plate). This has been observed in previous studies and can explain why no Cl_2 was detected when the (per)chlorates were in silica, as it may react with the water desorbed from the silica to form HCl, a phenomenon also observed in the Mars' EGA SAM flight data [12,18] and produced as follows:

$$2Cl_2 + 2H_2O \rightarrow 4HCl + O_2 \quad (1)$$

The pyrolysis of hydrated perchlorates leads to their thermal decomposition, preceding a dehydration phase associated to a sudden weight loss [42–45]. In this study, only the thermal decomposition of the oxychlorines was observed, as well as a dehydration phase for some of them. The dehydration of (per)chlorates, followed by the thermal decomposition of the Ca and Na perchlorates and of K and Na chlorates led to the production of O_2 and HCl formation through the following general reactions (X can be a Ca, N or K atom) [4]:

$$X^{Z+}(ClO_4)_Z{\cdot}nH_2O \rightarrow X^{Z+}(ClO_4)_Z + nH_2O$$

$$X^{Z+}(ClO_4)_Z \rightarrow XCl_Z + Z{\cdot}2O_2$$

The thermal decomposition of Fe perchlorate and Mg perchlorate include a dehydration phase and lead to the formation of oxide (O^{2-}) and

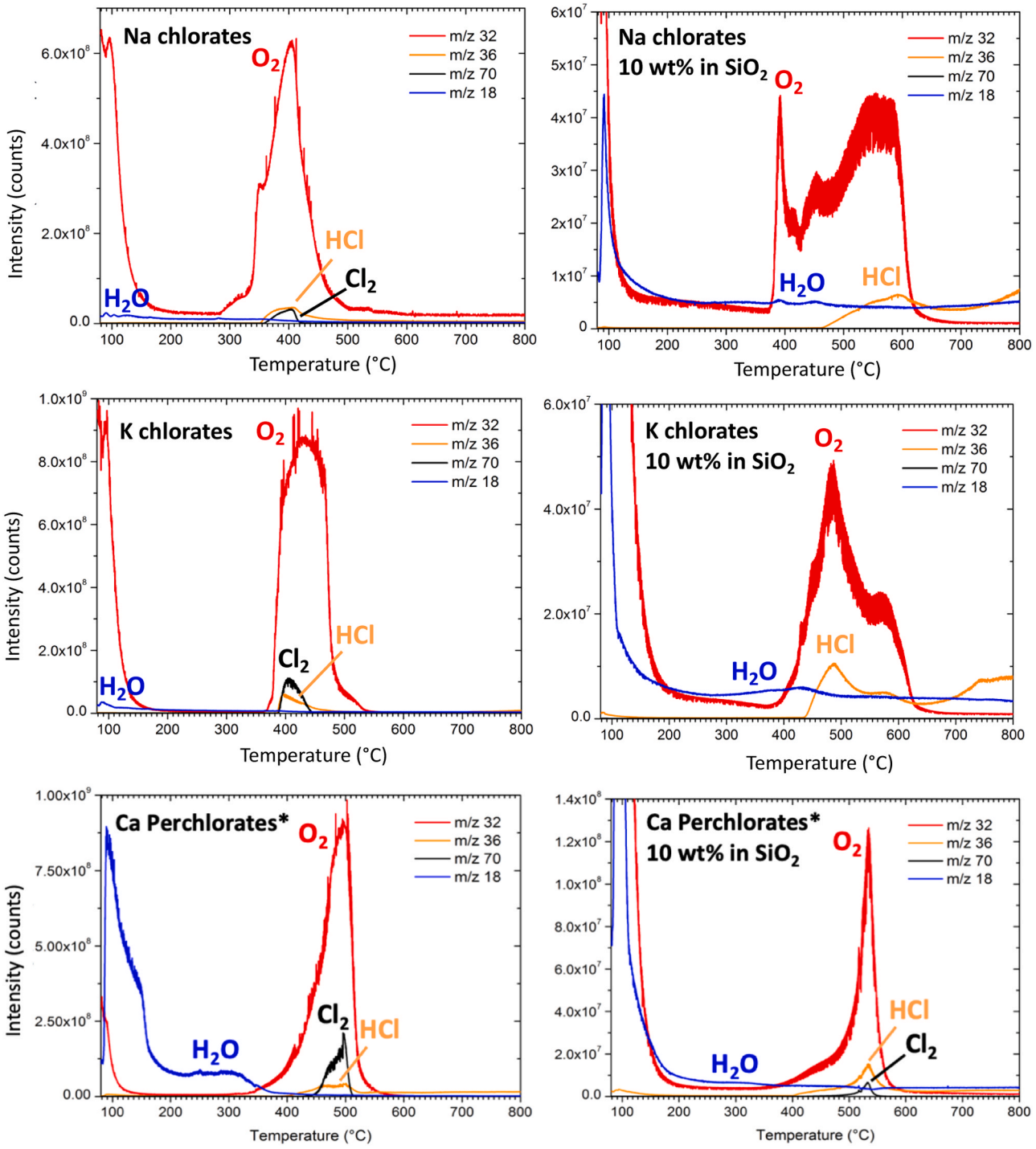

Fig. 1. Thermally evolved gas analyses of (left) pure (per)chlorates and (right) 10 wt% of (per)chlorate mixed in silica showing that more Cl_2 is released when (per) chlorate are pyrolyzed in pure form compared to when they are mixed in silica. *Published in [12] and plotted as a comparison with the other oxychlorine phases. Compounds are identified as followed: *m/z* 32: dioxygen (O_2), *m/z* 36: hydrochloric acid (HCl), *m/z* 70: dichlorine (Cl_2), and *m/z* 18: water (H_2O). Differences are observed within the range of releasing temperatures (90–800°C) of the species considered for each oxychlorine. The mass of (per)chlorate was the same in each case and equals to 0.5 mg.

Cl_2 according to the following reaction (X is an Fe (ferrous) or Mg atom):

$$2X(ClO_4)_2 \rightarrow 2XO + 7O_2 + 2Cl_2$$

The Cl_2 produced can then react with water vapor present in the system to form HCl. These reactions and the released species seen in our study are consistent with the species observed in the thermograms during the pyrolysis of pure (per)chlorates. However, these trends evolve when oxychlorines are mixed at 10 wt% in silica. The thermal decomposition of the oxychlorines and the volatiles released during pyrolysis are detailed below and compared to the literature.

3.1.1. *Mg perchlorate*

H_2O, O_2, HCl, and Cl_2 were released during the pyrolysis of Mg perchlorate despite the presence of silica, but their relative abundances

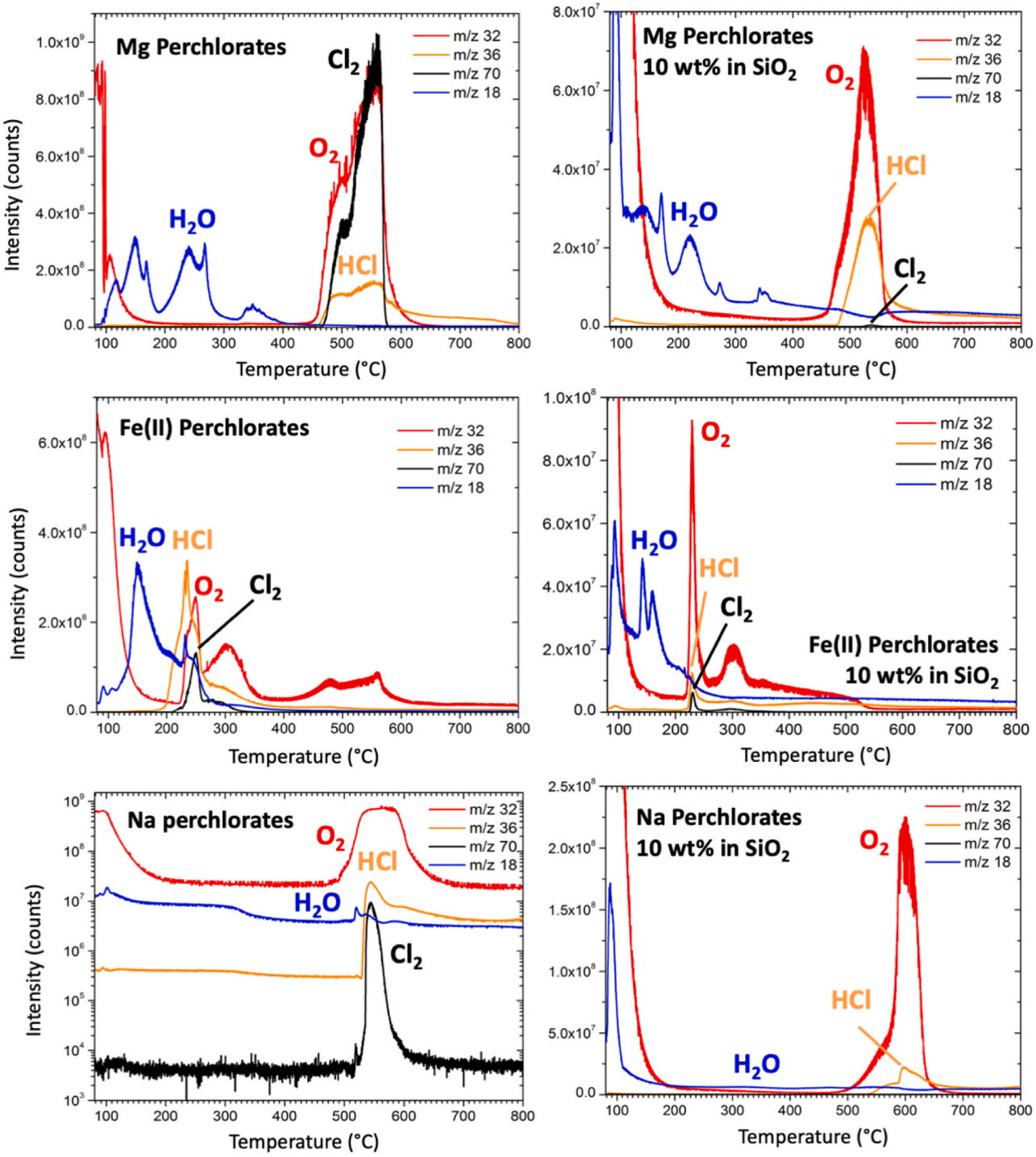

Fig. 1. (*continued*).

decreased of at least an order of magnitude with Cl_2 being the most impacted. Three H_2O release were observed in pure $Mg(ClO_4)_2$ and five in silica. The first peak was related to water desorbing from the silica whereas the others are likely related to water desorbing from $Mg(ClO_4)_2$ itself, although it was not hydrated. In silica, the H_2O release was 20°C higher compared to pure $Mg(ClO_4)_2$ and the temperatures shifted to a 20–30°C lower range (reverse trend compared to the other salts). Except for Cl_2, silica had less influence on Mg compared to Ca perchlorate and Na chlorate. The thermal evolution of Mg perchlorate during pyrolysis were consistent with the data from [43]:

1. At 170°C and 200°C, the two water releases are likely due to the hydrolysis of $Mg(ClO_4)_2$followed by dihydroxylation according to the following reactions:

$$Mg(ClO_4)_2{\cdot}6H_2O\ (solid) \rightarrow Mg(OH)_2\ (solid) + 2HClO_4\ (liquid) + 4H_2O\ (gas)$$

$$Mg(OH)_2\ (solid) \rightarrow MgO\ (solid) + H_2O\ (gas)$$

2. At 251°C, the dehydrated Mg perchlorate melts (not visible in EGA).

3. At 528°C, O_2 is released between 460 and 600±10°C and indicates the thermal decomposition of $Mg(ClO_4)_2$. This peak is correlated to the release of HCl and Cl_2 at 533°C and 535°C, respectively. Cl_2 can be produced from magnesium dichloride ($MgCl_2$) and O_2, via the reaction:

$$MgCl_2\ (solid) + 1/2\ O_2\ (gas) \rightarrow MgO\ (solid) + Cl_2\ (gas)$$

Beyond 427°C, Mg perchlorate was likely decomposed into Cl_2 and O_2 according to the reaction:

$$Mg(ClO_4)_2 \rightarrow MgO + Cl_2 + 7/2\ O_2$$

The O_2, Cl_2, and HCl released at high temperature were likely produced from the reaction above, since a large fraction of Cl_2 likely reacted with water from silica to produce HCl.

3.1.2. Fe(II) perchlorate (hydrated)

An important water release was observed during the pyrolysis of Fe $(ClO_4)_2$ in the absence (two peaks at 148°C and 233°C) and in the presence of silica (three peaks at 92°C, 142°C, and 157°C). The behavior of $Fe(ClO_4)_2$ is similar to $Mg(ClO_4)_2$, with an increase in the relative abundance of H_2O in silica likely related to its hydration state. O_2 is released at 250°C, 300°C, and between 450°C-580°C for pure $Fe(ClO_4)_2$ and at 230°C and between 300°C-530°C in silica, a shift to lower temperatures observed for Mg perchlorate. HCl did not track Cl_2 when Fe $(ClO_4)_2$ was pyrolyzed pure. In the presence of silica, the intensities are decreased by 10–100. $Fe(ClO_4)_2$ is not well described in the literature compared to the other salts considered but metallic perchlorates are known to thermally decompose through similar reactions [43], likely as follows:

1. At 142°C and 157°C, two peaks of water were observed are likely related to the dehydration of $Fe(ClO_4)_2$ via the reaction:

$$Fe(ClO_4)_2 \cdot nH_2O \rightarrow Fe^{2+}\ (ClO_4)_2 + nH_2O$$

The hydrolysis of the remaining water incorporated in the mineral likely happened through the reaction:

$$Fe(ClO_4)_2 \cdot nH_2O \rightarrow Fe(OH)_2\ (solid) + 2HClO_4 + (n\text{-}2)H_2O$$

2. At 230°C, O_2, HCl, and Cl_2 were sharply released, which is consistent with the thermal decomposition of Fe perchlorate via the reaction:

$$2Fe(ClO_4)_2 \rightarrow 2FeO + 2Cl_2 + 7O_2$$

3. At 300±20°C, some O_2 is again released and progressively decreased down to 540°C. This last is correlated to a low HCl and Cl_2 release which are likely produced from reaction (1). The continuous production of O_2 in addition to the release of HCl and Cl_2 could be related to a balance effect through the following reversible reaction [43]:

$$FeO\ (solid) + Cl_2\ (gas) \leftrightharpoons FeCl_2\ (solid) + ½\ O_2\ (gas)$$

3.1.3. Na perchlorate

All species except Cl_2 were released when Na perchlorate was pyrolyzed in silica with peaks shifted ~40°C to higher temperatures. However, the release temperatures of the species and their intensities were within the same order of magnitude. $Na(ClO_4)_2$ had a similar behavior as $Ca(ClO_4)_2$ [12] and its thermal decomposition steps can be extrapolated from the pyrolysis of $Ca(ClO_4)_2$:

1. At 130°C, $Na(ClO_4)_2$ melted, a process not visible in EGA.
2. At 600±10°C, O_2 was released as well as HCl with a slight shoulder around 560±5°C. This release likely indicates the thermal decomposition of $Na(ClO_4)_2$ according to the following reaction:

$$NaClO_4\ (solid) \rightarrow NaCl\ (solid) + 2O_2\ (gas)$$

3.1.4. Na and K chlorates

The thermal behaviors of Na and K chorates were relatively similar. The release of Cl_2 was inhibited in silica, the temperature releases shifted to higher temperatures (~100°C) and all the intensities decreased by at least one order of magnitude. Results are consistent with the thermal decomposition of Na and K chlorates [46,47]:

1. At 263°C and 256°C, $Na(ClO_3)$ and $K(ClO_3)$ melted, respectively (not visible in EGA).
2. In $Na(ClO_3)$, two H_2O releases were observed at 389±5°C and 450 ±5°C, and one at 428°C±10°C which likely correspond to the dehydration steps of $Na(ClO_3)$ and $K(ClO_3)$.
3. The O_2 peaks observed at 391°C for $Na(ClO_3)$ and at 480 and 570°C for $K(ClO_3)$ are likely correlated to their thermal decomposition following the reaction (with X the Ca or K atom):

$$2XClO_3\ (solid) \rightarrow 2XCl\ (solid) + 3O_2\ (gas)$$

4. HCl was released from 595°C to 800°C in $Na(ClO_3)$ and 440–800°C in $K(ClO_3)$, in correlation with O_2 release which are likely produced together during reaction (1).

3.1.4.1. Discussion. The temperature releases of the volatiles for each salt are summarized in Figure S1. The thermograms obtained after the pyrolysis of the salts mixed in silica (10 wt%) indicated peak shifts to higher temperatures (from 30°C to 100°C) compared to the analyses of pure salts. This trend was reversed for the metallic Mg and Fe perchlorates. Except for Na perchlorate, the intensities of the peaks were decreased by a factor 10 up to 100 in silica. The release of Cl_2 seemed inhibited by the silica during the pyrolysis of Na / K chlorates and Na perchlorates and the abundance of HCl was relatively higher for all the salts studied. The silica absorbed part of the heat from the pyrolyzer during the release of the species, thus the diffused heat increased the temperature release of most species which took more time to extract themselves from the sample, as observed in previous studies [12,48]. Mg and Na perchlorates were the least affected by silica likely because they decomposed at higher temperature (> 500°C) compared to the other salts. For the rest of the paper, we will only discuss the temperatures of the species released in the presence of silica since both salts and organics were mixed in silica for the pyr-GC/MS analyses.

The main volatiles O_2, HCl, and Cl_2, released at various temperatures depending on the salt during pyrolysis, can then react with the organic molecules. Fe perchlorate decomposed at the lowest temperature (~230°C), followed by Na chlorate (~390°C), K chlorate (~480°C), Mg perchlorate (~530°C), Ca perchlorate (~540°C), and Na perchlorate (~600°C). Water can indirectly interact with organic matter through hydrolysis reactions and lead to the formation of HCl if it is released in sufficient amounts. Water was released at different temperatures in the case of Fe and Mg perchlorates. From Markowitz, 1963, and Marvin and Woolaver, 1945, the final residue obtained after heating Ca and Na perchlorates, and Na and K chlorates, are calcium, sodium and potassium chlorides (CaCl, NaCl and KCl). The final residue of Fe and Mg perchlorates are iron oxides (Fe_2O_3) and magnesium oxide (MgO), or a mixture of MgO magnesium chloride and $MgCl_2$. These residues could also react with the organic molecules present in martian samples, especially if they are released at similar temperatures as the species released from the salts. Silica is highly hygroscopic and thus has a high

absorption capability. As observed in EGA, absorbed water can react with chloride compounds such as Cl_2 and indirectly play a role on the chlorination of the organics through the production of HCl.

3.2. Influence of the fused silica matrix on the flash-pyrolysis of PAHs

As shown above, silica can influence the release and decomposition of the species. In order to characterize the potential influence of silica on the pyrolysis of PAHs and obtain referential data prior to evaluating the influence of salts on PAHs, they were also pyrolyzed in pure form and in silica, using the same concentration as the oxychlorines-organics mixture (see the representative chromatogram of naphthalene in Fig. 2 as an example). We note that silica was pyrolyzed in pure form and no major contaminants were detected [12].

Results indicated that the nature and number of pyrolyzates were similar whether silica was present or not. Minor quantitative differences were observed, however, such as a higher abundance of the parent molecule and its high molecular weight pyrolyzates ($> C_{10}$) in silica compared to pure PAHs (Fig. 2) as well as slightly longer elution times ($\sim$ 0.3 min). This is consistent with the fact that silica may delay the heating and subsequent outgassing of the organics [12]. The higher relative abundance of naphthalene's pyrolyzates ($> C_{10}$) is consistent with a minor catalytic effect of silica that may have favored the chemical reactions generally induced by high pyrolysis temperature such as cyclization, aromatization, and recombination of the pyrolyzates. Similar results were obtained with phenanthrene, and benzanthracene and chromatograms were therefore not displayed. In conclusion, PAHs are thermally stable and mostly decomposed into stable aromatic pyrolyzates which were not qualitatively affected by the silica.

Therefore, silica was kept as a solid matrix for dilutions to introduce a low concentration of organic molecules and salts in order to protect the instrument and limit contamination and carry-over between the analyses, and to dilute the organics and salts as they would be on Mars. Although not completely representative of the sample mineralogy analyzed by SAM, silica has been detected at the surface of Mars including in Gale crater [38,39] and at Columbia Hills and is thus a relevant mineral martian analog. Silica has also been suggested as a mineral with high organic and biosignature preservation potential [49–51].

3.3. Pyrolysis of PAHs mixed in silica

The second step consisted in investigating the nature, number, and structure (*i.e.*, aromatic or aliphatic) of the molecules formed during the flash-pyrolysis of PAHs in silica to shed light on their formation mechanisms. To ensure repeatability, analyses were reproduced two to three times and no major qualitative nor quantitative differences were observed.

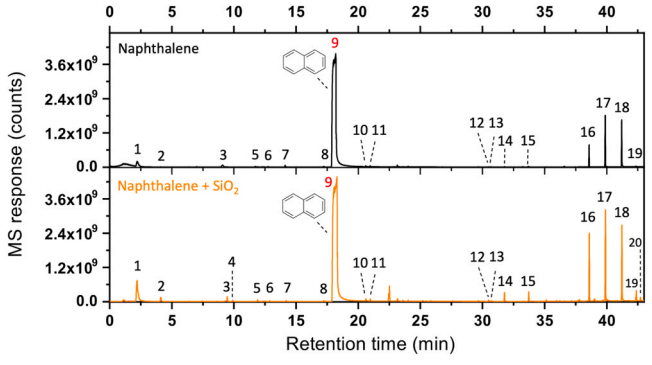

Fig. 2. Chromatograms obtained after the pyrolysis of ~0.15 mg of pure naphthalene (black) compared to 0.5 wt% of naphthalene mixed in fused silica (orange). The highest abundance compounds that were detected correspond to: 1. CO_2, 2. benzene, 3. phenylethyne, 4. styrene, 8. methylene-indene, 9. naphthalene (parent molecule), 10. 2-methylnaphthalene, 11. 1-methylnaphthalene 12. phenanthrene, 13. anthracene, 14. vinylanthracene, 15. phenylnahpthalene, 16. triphenylene, 17. 1,1-binaphthalene, 18. 1,2-binaphthalene, 19. benzofluoranthene, and 20. dinaphthofurane.

The main compounds released during the pyrolysis of naphthalene ($C_{10}H_8$), phenanthrene ($C_{14}H_{10}$), and benzanthracene ($C_{18}H_{12}$) are represented in Fig. 3. The nature of all pyrolyzates can be found in the Supplemental Materials (Table S1). Results indicate that the main pyrolysis products are the parent PAHs themselves alongside with aromatic compounds, which is consistent with previous studies (Moldoveanu, 2009). The number and relative abundances of pyrolyzates decreased with the increase of the size of the molecule (Fig. 3). This is likely due to an increase in the thermal and chemical stability of the molecule driven by the number of carbon rings. The detection of aromatic compounds of lower molecular weight than the parent molecule (e.g., styrene, benzene, toluene) can be explained by a higher energetic input compared to the dissociation energy of the aromatic C-H bonds causing the rupture and isolation of the rings. Aromatic compounds with higher molecular weights than the parent molecule were present. The number of high molecular weight compounds increased accordingly with the size of the pyrolyzed molecule. The PAHs formed during pyrolysis have coplanary and non-coplanary rings. During pyrolysis, regardless of the number of rings, the formation mechanisms of the compounds are similar to those formed during the pyrolysis of benzene (C_6H_6, one ring) and toluene (C_7H_8, one ring attached to a methyl group). Endothermic processes play a role with successive dehydrogenation steps leading to the formation of biphenyl during the pyrolysis of benzene [52]. In the case of naphthalene, the first process is the formation of naphthyl radicals. The naphthyl radical reacts with naphthalene, further liberating the H• radical and producing the 1, 2-binaphthalene and associated isomers observed in our analyses (Fig. 3 and Table S1). The formation of this coplanery structures weaken the covalent bonds and cyclodehydration reactions can happen. They tend to stabilize themselves by forming coplanery molecules such as benzofluoranthene, which was detected after the pyrolysis of naphthalene and phenanthrene. The formation of molecules with 5–6 carbon rings was likely, but their low volatility and high retention time likely prevented their detection in our analytical conditions. The formation of high molecular weight pyrolyzates at high temperature may also lead to the production of soot, with a basic structure of more than 50 carbon rings which is unresolved with GCMS [52].

Results also revealed the release of a few oxygen-bearing molecules including heterocycles (e.g., benzofurane), aldehydes (e.g., benzaldehyde), and ketones (e.g., naphthoquinone) with molecular weights consistent with the size of the parent PAH (Fig. 3 and Table S1). A possible explanation is that the oxygen from the silica matrix (SiO_2) induced the oxidation of the PAHs through the following redox reaction: $2\,C + SiO_2 = Si\ (solid) + 2\,CO$. Another hypothesis is the adsorption/desorption of water from the silica which was subsequently cleaved into free radicals (H^+ and HO^+) that reacted with the pyrolyzates [48]. The formation of high molecular weight hydrogenated compounds such as dihydronaphthacene, was also observed. Although their formation process is generally unknown, these compounds may have formed by hydrogenation from the H_2 formed during pyrolysis or during the dehydration and dehydrogenation of the water present within the silica matrix.

In conclusion, PAHs have a high thermal stability and did not entirely decompose despite the high pyrolysis temperature used (850°C). They generated lighter and heavier molecular weight aromatic hydrocarbons compared to the parent PAH, with the majority of compounds common to all three PAHs. Although it can be difficult to identify a PAH from its pyrolyzates, their high thermal stability, even when present in low concentrations, indicate that they should be detectable and identifiable in a martian sample depleted of reactive species. However, PAHs are very reactive and strongly reacted with the traces species present in the system (O_2). Results also indicate that the relative

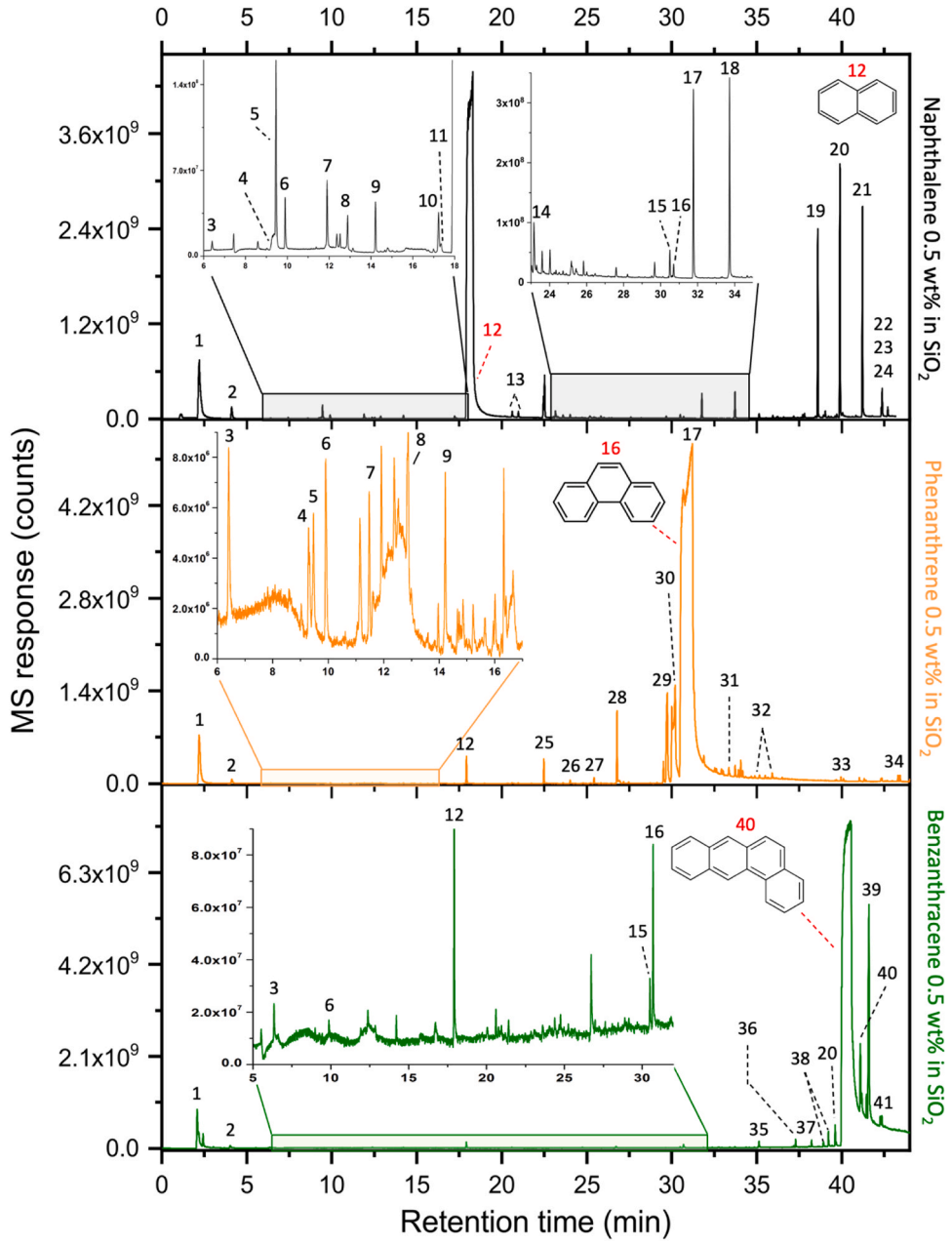

Fig. 3. Chromatograms obtained after the pyrolysis of the PAHs mixed in fused silica at 0.5 wt%: naphthalene (black), phenanthrene (orange) and benzanthracene (green). Only the major compounds were represented on the figure and include: 1: CO_2, 2: benzene, 3: toluene, 4: xylene, 5: phenylethyne, 6: styrene, 7: benzaldehyde, 8: benzofurane, 9: indene, 10: methylene-indene, 11: phenylbutenyne, 12: naphthalene, 13: methyl-naphthalene isomers (2), 14: naphthoquinone, 15: phenanthrene, 16: anthracene, 17: vinylanthracene, 18: phenylnaphthalene, 19: triphenylene, 20. 1,1-binaphthalene, 21. 1,2-binaphthalene, 22: benzofluroanthene, 23: benzopyrene-oxide, 24: dinaphthofurane, 25: biphenyle, 26: biphenylene, 27: acenaphthylene, 28: fluorene and phenalene isomers, 29: fluorenone, 30: phenalenone, 31: anthraquinone, 32: pyrene and fluoranthene isomers, 33: binaphthalene isomers, 34: diphenylphenanthrene and diphenylanthracene, 35: benzofluroene, 36: dihydronaphthacene, 37: benzofluorenone, 38: benzanthracene, 39: chrysenol, 40: naphthacene, and 41: naphthacenequinone. The compounds in red correspond to the parent molecules.

abundances of low molecular weight pyrolysis fragments (e.g., benzene and toluene) decreased as the size of the molecules increased, underscoring that the thermal and chemical stability of PAHs increases with size, as expected. The presence of oxygen-bearing molecules of the same number of carbons as the PAH pyrolyzed indicates that the molecular reactivity did not depend on the size of the parent molecule.

We showed that flash-pyrolysis is an efficient technique to extract PAH from a sample. However, the martian regolith is not inert and contains complex mineral assemblages that may impact the organic molecules during pyrolysis such as clays, sulfates, iron oxides, chlorides, perchlorates, and chlorates [5,8,53–55]. Following-up on studies that have focused on the influence of these minerals on martian analog soils and organics during pyrolysis [12,14,41,48,56–63], we investigated the influence of six oxychlorine phases on PAHs and discuss their (oxy) chlorination processes and the formation of chlorohydrocarbons and oxygen-bearing compounds.

3.4. *Influence of the type of salts on the flash-pyrolysis of PAHs*

Throughout this study, two questions will be systematically discussed for each PAH:

1. Do oxychlorine minerals degrade the parent molecule and/or its pyrolyzates?
2. What are the nature and relative abundances of the oxidized, chlorinated, and/or oxychlorinated organic compounds formed during pyrolysis?

To answer these questions, the number and the nature of pyrolyzates generated, including oxidized, chlorinated, and oxychlorinated compounds, were evaluated (Fig. 4 and Table 2) considering only the compounds that had a signal/noise ratio $\geq 3\sigma$ in the TIC. The relative abundances of the parent molecules was also evaluated on selected thermal decomposition products.

The chromatogram obtained after the pyrolysis of naphthalene in the presence of calcium perchlorate $Ca(ClO_4)_2$, iron perchlorate $Fe(ClO_4)_2$, and potassium chlorate $K(ClO_3)$, are presented in Fig. 5 (major compounds noted). The complete list of pyrolyzates can be found in Table S2.

3.4.1. Naphthalene

The relative abundance of naphthalene did not decrease in the presence of Ca, Fe, or Na perchlorates, or Na chlorate, compared to naphthalene in silica. The relative abundance decreased within the same order of magnitude with K chlorate but decreased significantly (by two orders of magnitude) with Mg perchlorate.

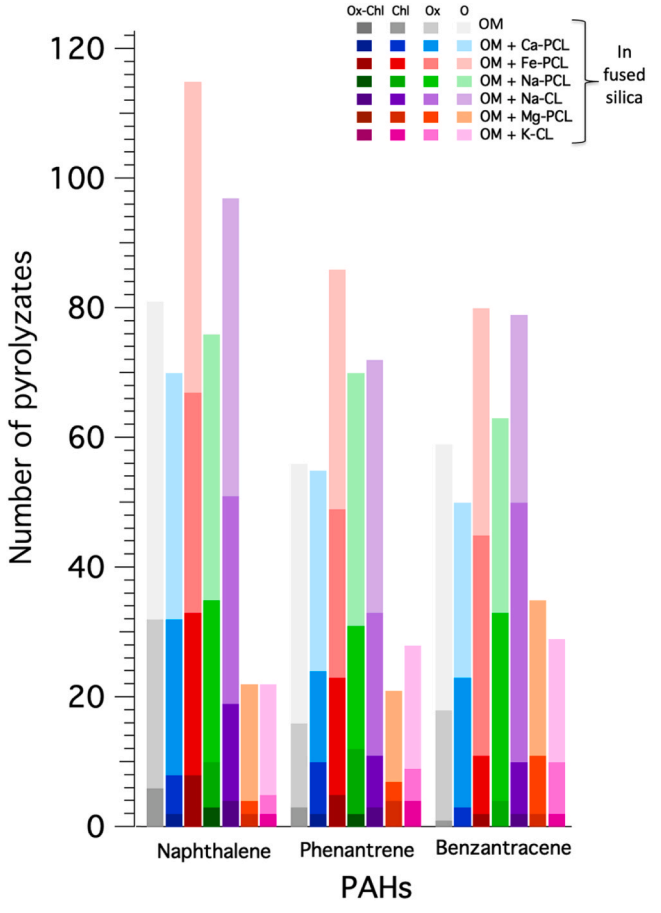

Fig. 4. Statistical estimation of the number of compounds detected after the flash-pyrolysis of each PAH in fused silica (0.5 wt%) and mixed with the six oxychlorine phases. For each parent molecule, the number of detected compounds is represented by a color: gray: PAH in fused silica; blue: PAH + Ca perchlorate; red: PAH + Fe perchlorate; green: PAH + Na perchlorate; purple: PAH + Na chlorate; orange: PAH + Mg perchlorate and pink: PAH + K chlorate. The four nuances of color (darkest to lightest) represent the chemical family of the pyrolyzates: Ox-Chl: oxychlorinated compounds, Chl: chlorine-bearing compounds, Ox: oxygen-bearing compounds. The compounds that did not belong in these three categories were named "O" for "Others" (lightest color). All the compounds were mixed in Fused Silica (FS).

The number of pyrolyzates varied depending on the analysis as shown in Figs. 4 and 5, and Table 2. Most of the aromatic compounds formed during the pyrolysis of naphthalene in silica were still present after pyrolysis with Ca and Fe perchlorates and Na chlorate. Aromatics included compounds of lower and higher molecular weight compared to naphthalene such as benzene, toluene, the xylene isomers, phenylethyne, styrene, the methyl-naphthalene isomers, phenanthrene and anthracene, the vinyl-anthracene and phenanthrene isomers, biphenyl, acenaphthylene up to triphenelyne, and benzanthracene.

The peak areas of three pyrolyzates systematically detected were measured as follows: benzene (4.1 min), indene (14.2 min) and phenanthrene (30.5 min). The area of benzene increased of an order of magnitude in the presence of Ca and Fe perchlorate and was three times higher with Na chlorate. The areas of indene and phenanthrene increased of an order of magnitude with Fe perchlorate. Fe perchlorate and Na chlorate seemed to react preferentially with the parent molecule rather than its pyrolyzates, as showed by the similar relative abundances of the compounds regardless the presence of oxychorines. The compounds formed during the pyrolysis of naphthalene in silica also formed with Fe perchlorate whereas Ca perchlorate appeared to react with dozens of molecules. In the presence of Ca perchlorate, the alkyl-bearing molecules from the thermal decomposition of naphthalene—likely more fragile—were not present. This could be due to the substitution of the alkyl group by chlorine, although there were less chlorinated-bearing molecules in the presence of Ca perchlorate compared to Fe perchlorate.

The pyrolysis of naphthalene in the presence of Ca and Fe perchlorates led to the formation of numerous oxidized, chlorinated, and oxychlorinated compounds (Figs. 4 and 5, Table 2). More oxidized compounds were detected with Fe perchlorate compared to Ca perchlorate. The aromatic chlorohydrocarbons included chlorobenzene, the two chloronaphthalene isomers, three dichloronaphthalene isomers, one dichlorophenanthrene isomer, dichloromethylenefluorene, chloronaphtoquinone, and likely cinnamoylchloride. With Fe perchlorate, the number of chlorinated aromatic compounds (33), oxychlorinated (8), and oxidized compounds (36) increased drastically in comparison to Ca perchlorate, with relative abundances up to a hundred times higher. Some (oxy)chlorinated compounds were detected only in the presence of Fe perchlorate: dichlo-, trichlo- and tetrachlorobenzene, the trichloronaphtalene isomers, chlorophenylethylene, chlorophenol isomers, dichlo- and trichlorophenol isomers, chlorobenzaldehyde, and chlorobenzofurane. Two chlorinated aliphatics were detected, trichloroethylene and tetrachloroethylene. Three dichloroethylene isomers were also found by searching for their major ion mass fragment.

Na chlorate strongly reacted with naphthalene as shown by the numerous oxidized (34) and (oxy)chlorinated compounds (22) detected which were similar to those detected with Fe perchlorate (Table S2). The oxidized compounds were mostly aldehydes (e.g., benzaldehyde, two naphtaldehyde isomers), aromatic/aliphatic alcohols (e.g., phenol, naphthalenol), and oxygen-bearing heterocycles (e.g., phenalenone, benzofurane and naphthacenequinone). Similarly, the chlorinated compounds formed after the pyrolysis of naphthalene with Na chlorate were the same as with Fe perchlorate except that all the dichloronaphthalene isomers were present with Fe perchlorate. Cinnamoylchloride, chlorobenzaldehyde isomers, chloronaphthaquinone, and chlorothioxanthenone were also detected. The chlorohydrocarbons were present in lower abundance (~an order of magnitude) in the presence of Na chlorate compared to Fe perchlorate. The high number of oxidized and (oxy)chlorinated compounds indicates the action of (oxy)chlorination and oxidation of the perchlorates on naphthalene and its thermal decomposition products. Fe perchlorate and Na chlorate had a stronger impact compared to Ca perchlorate as shown by the number and relative abundances of (oxy)chlorinated and oxidized pyrolyzates.

Na and Ca perchlorates had a similar behavior and reacted with

Table 2
Number of compounds detected after pyrolysis of the three PAHs mixed in silica and in the presence of the perchlorate and chlorate salts. The number of pyrolyzates was separated in three categories: the total number of compounds detected (T) which includes: the number of oxygen-bearing compounds (Ox), chlorine-bearing compounds (Cl), and oxygen/chlorine-bearing compounds (Ox-Cl). Darker shading indicates higher numbers of pyrolyzates.

	PAH in fused silica (0.5 wt%)		PAH + Ca-PCL in fused silica			PAH + Fe-PCL in fused silica			PAH + Na-PCL in fused silica			PAH + Na-CL in fused silica			PAH + Mg-PCL in fused silica			PAH + K-CL in fused silica		
Pyrolyzates / Organic molecule	T	Ox	T	Ox	Cl/ Ox-Cl	T	Ox	Cl/ Ox-Cl	T	Ox	Cl/ Ox-Cl	T	Ox	Cl/ Ox-Cl	T	Ox	Cl	T	Ox	Cl
Naphthalene	71	19	77	28	8/2	127	36	33/8	84	29	8/3	106	34	18/4	28	2	4	27	4	4
Phenanthrene	61	13	61	15	11/3	100	26	26/7	77	19	15/2	81	22	11/4	22	3	6	24	5	5
Benzanthracene	59	17	60	23	5/0	88	34	16/2	70	31	6	71	40	12/2	40	10	2	30	9	2

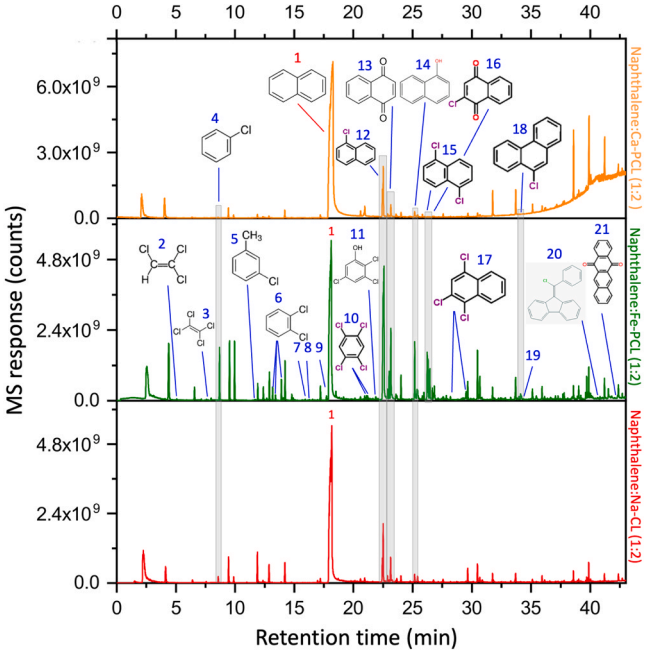

Fig. 5. Chromatograms obtained after the pyrolysis of naphthalene mixed with 1 wt% of calcium perchlorate (orange), 1 wt% of iron perchlorates (green), and 1 wt% of sodium chlorate (red). Only the "modified" compounds and the parent molecule have been identified as follows 1: naphthalene, 2: trichloroethene, 3: tetrachloroethene, 4: chlorobenzene, 5: 2x chlorotoluene isomers, 6: 3x dichlorobenzene isomers, 7: 2x chlorobenzalehyde isomers, 8: 3x trichlorobenzene isomers, 9: dichlorophenol, 10: 2x tetrachlorobenzene isomers, 11: trichlorophenol, 12: 2x chloronaphthalene isomers, 13: naphthoquinone, 14: naphthalenol, 15: 3–4 dichloronaphthalene isomers (depending on the salt), 16: chloronaphtoquinone, 17: 3x trichloronaphtalene isomers, 18: chlorophenanthrene and chloroanthracene isomers (only one isomer in calcium perchlorate), 19: chlorovinylanthracene, 20: chloro(phenyl)methylenefluorene, 21: naphthacenedione.

naphthalene and its pyrolyzates to form ~30 oxidized and ~10 (oxy) chlorinated compounds. Their nature was similar as those formed with Fe perchlorate and Na chlorate but they were released in lower abundances. For example, the abundance of chlorobenzene was 50 times lower with Na chlorate and Ca perchlorate compared to Fe perchlorate. Na perchlorate and Ca perchlorate thus had a similar reactivity with naphthalene in terms of oxidation and (oxy)chlorination.

Mg perchlorate and K chlorate reacted similarly with naphthalene (Fig. 4, Table 2 and S2) with only ~30 compounds formed: naphthalene and aromatic hydrocarbons but in lower abundance compared to pyrolysis with other oxychlorine phases. Since only a few chlorinated and oxidized compounds were detected, Mg perchlorate and K chlorate appeared to react with only a portion of naphthalene and its pyrolyzates to form molecules that were unlikely detectable in our analytical conditions. Mg perchlorate and K chlorate seemed to oxidize/chlorinate or induce the total combustion of naphthalene.

3.4.2. *Phenanthrene*

Phenanthrene and benzanthracene had a similar behavior as naphthalene regarding the oxychlorines, and therefore their chromatograms are not displayed but the number and nature of pyrolyzates formed are presented in Fig. 4 and Table S2. Phenanthrene was detected in all the chromatograms, regardless of the nature of the oxychlorine. By measuring the relative abundance of phenanthrene, we were able to rank the salts from the most to least reactive with phenanthrene. In the presence of Ca and Na (per)chlorate, the areas of phenanthrene decreased by ~5, with Fe perchlorate, by 2, and with Mg perchlorate and K chlorate, the areas were 1000 and 35 times lower, respectively. Mg perchlorate thus had the strongest impact since it degraded phenanthrene almost entirely, followed by K chlorate, Ca and Na perchlorate, and Na chlorate and Fe perchlorate.

The number of pyrolyzates detected followed the trend of naphthalene (Fig. 4 and Table 2). ~61 compounds were detected after the pyrolysis of phenanthrene in silica and in the presence of Ca perchlorate. This number increased with Fe perchlorate, Na perchlorate, and Na chlorate to 100, 77, and 80 compounds, respectively, and decreased drastically in the presence of Mg perchlorate and K chlorate. Aromatic hydrocarbons resulting from the thermal decomposition of phenanthrene were also systematically detected. A few oxidized compounds that were previously detected in silica only were also detected but in much higher amounts. However, higher molecular weight PAHs decomposed in higher molecular weight compounds regardless of the presence of salts. The relative abundances of a few compounds (e.g., benzene) were consistent with the degradation of the parent molecule by the salts. In the presence of Na perchlorate, the abundance of benzene was relatively similar to phenanthrene in silica whereas it was two, three and ten times higher with Na chlorate, Ca perchlorate, and Fe perchlorate, respectively. A similar trend was observed for the other pyrolyzates. Mg perchlorate and K chlorate seemed to react with most of the pyrolyzates. Na chlorate, Ca perchlorate, and Fe perchlorate reacted preferentially with phenanthrene and/or reacted less with its pyrolyzates, contrary to the other oxychlorine phases.

The increase in the number of pyrolyzates formed with Fe and Na (per)chlorates is consistent with the formation of new oxidized and (oxy)chlorinated compounds (Table S2). Some organo-chlorinated compounds typical of phenanthrene were identified including chloroanthracene, chlorophenanthrene, and chlorobiphenyl, resulting directly from the chlorination of phenanthrene and its pyrolyzates by

the salts. Because they were detected in all the analyses, these compounds would not be able to help identify the nature of the salt originally present in the sample. However, they can help identify the nature and the size of the parent PAH (though not the nature of the isomer). The nature of the (oxy)chlorinated compounds formed were similar after the pyrolysis of phenanthrene with all the perchlorates.

A few oxidized compounds were detected specifically with Fe and Na (per)chlorate. Those compounds include aldehydes, alcohols, and oxygen-bearing heterocycles such as ketones and phthalic acid anhydride which has been interpreted as a likely contamination in previous studies [12]. The oxygen-bearing compounds detected are consistent with the oxidation of phenanthrene and its pyrolyzates by the salts. Anthraquinone was detected with naphthalene only and resulted from the direct oxidation of phenanthrene. Phenanthropyrane was detected only with Fe and Na (per)chlorates. The detection of anthraquinone and phenanthropyrane in a martian sample could therefore help identify phenanthrene and potentially the types of salts after pyrolysis. An equivalent number of oxidized compounds was detected after the pyrolysis of phenanthrene in silica and with Ca perchlorate, so the oxidation impact of Ca perchlorate is probably not significant.

To conclude, the thermal behavior of phenanthrene in the presence of salts was similar to naphthalene. Fe perchlorate had a stronger oxidation and (oxy)chlorination impact followed by Na chlorate and Na perchlorate. Ca perchlorate favored the formation of chlorinated compounds but not oxidized compounds. Mg perchlorate and K chlorate were the most destructive. Ca / Fe perchlorates and Na chlorate reacted preferentially with phenanthrene rather than its pyrolyzates. This hypothesis is supported by the increase of the relative abundances of the pyrolyzates (mostly aromatic hydrocarbons) usually formed during the pyrolysis of phenanthrene in silica. Fe perchlorate and Na chlorate only needed a small portion of pyrolyzates to form the oxidized and chlorinated compounds detected since all usual pyrolyzates were still detected in their presence.

3.4.3. Benzanthracene

The number and nature of the compounds detected after the pyrolysis of benzanthracene with the six oxychlorine phases are presented in Fig. 4 and Table S2. Benzanthracene was detected in all the analyses with the salts except with Na chlorate. The peak area of benzanthracene in silica was similar in the presence of Mg perchlorate and decreased by two in the presence of Ca perchlorate and Na chlorate and by three and four with Fe and Na perchlorates, respectively. Na chlorate degraded entirely benzanthracene, followed by Na, Fe and Ca perchlorates, K chlorate, and finally Mg perchlorate, which did not react with benzanthracene.

The number of pyrolyzates detected was proportional to the number of pyrolyzates detected after the pyrolysis of phenanthrene with and without salts (Fig. 4 and Table 2). The same aromatic hydrocarbons and relative abundances were observed as with the other PAHs.

The nature, number, and relative abundances of chlorohydrocarbons were similar after the pyrolysis of benzanthracene with Fe perchlorate (18) and Na chlorate (14) and included chlorobenzene, the dichlorobenzene isomers, chloroethynylbenzene, trichlorobenzene, one chlorophenanthrene isomer and likely chloropyrene. Chloroanthraquinone, chlorobenzoanthracenone, and chloroundecane were detected only with Fe perchlorate and Na chlorate.

In the presence of Na perchlorate, four chlorohydrocarbons were produced: chlorobenzene, the dichlorobenzene isomers (ten times lower in abundance compared to Fe perchlorate and Na chlorate), chloroindenylideneindene, and chloroundecane. Ca / Mg perchlorates and K chlorate also led to the formation of chlorobenzene and the dichlorobenzene isomers but in lower abundance compared to Fe perchlorate and Na chlorate. Chloroindenylideneindene was detected in all the analyses except Na chlorate. No oxychlorinated compounds were detected with Ca, Na and Mg perchlorates nor K chlorate.

The highest number of oxygen-bearing compounds was detected in the presence of Na chlorate, followed by Fe perchlorate and Na perchlorate with ~40, ~34 and ~31 compounds, respectively. Ca perchlorate led to the formation of ~23 oxidized molecules, which is slightly above the number of oxidized compounds detected after the pyrolysis of benzanthracene in silica only (~17). The number of oxidized compounds decreased down to 10 and 9 in the presence of Mg perchlorate and K chlorate, respectively, and included aldehydes (e.g., benzaldehyde and its alkyled derivatives), alcohols (e.g., chrysenol, phenol), heterocycles and ketones such as benzofuran and its alkyled derivatives (only with Fe perchlorate and Na chlorate), and benzocyclobutenone. New O-bearing compounds were detected with the salts: benzonaphtofuran, dibenzofuran, phenylbenzofuran, benzanthrenone, benzofluorenone, naphthofuranone, xanthone, benzoxanthene, and naphtoquinone, as well as two carboxylic acids: phthalic acid anhydride and carboxylic acid-anthraquinone.

The salts behaved slightly differently with benzanthracene compared to naphthalene and phenanthrene. The new compounds were consistent with the (oxy)chlorination of benzanthracene and its pyrolyzates by Fe and Na perchlorates, and K chlorate. The few chlorohydrocarbons formed in presence of the other salts indicated their low chlorination influence on benzanthracene. The disappearance of benzanthracene in addition to the high number and relative abundances of oxidized and chlorinated compounds after pyrolysis with Na chlorate showed it had the strongest influence on benzanthracene of all the salts targeted. Although Fe and Na perchlorates formed a high number of (oxy)chlorinated and oxidized compounds, they did not influence benzanthracene and its pyrolyzates as much. Indeed, they only needed a low amount of gas to form the high number of chlorinated and oxidized compounds detected, again suggesting high reactivity. In conclusion, the influence of Ca / Mg perchlorates and K chlorate was similar as with naphthalene and phenanthrene. Ca perchlorate had the lowest influence, whereas Mg perchlorate and Na chlorate reacted with most of benzanthracene's pyrolyzates. The newly formed compounds were characteristic of benzanthracene and its pyrolyzates and their (oxy)chlorination and oxidation by the salts.

3.4.4. Discussion: influence of the salts on PAHs

The perchlorate and chlorate salts had a minor influence on PAHs as shown by the detection of the parent molecule in most of the chromatograms after pyrolysis. Fe perchlorate had the strongest chemical influence of all the salts targeted as indicated by the high number of chlorinated and oxidized compounds formed after pyrolysis. These compounds were produced through oxidation and (oxy)chlorination of the PAHs and their thermal decomposition products, with some pyrolyzates characteristic of the parent molecule. Despite the influence of the salts, the presence of certain compounds on Mars could help identify the parent molecule if PAHs were present: for example, the presence of chlorophenanthrene would strongly suggest the presence of phenanthrene in a sample.

The reactivity of PAHs with the salts allowed to rank their influence and capability to degrade them and their pyrolyzates and/or react to form new compounds. In decreasing order, Fe perchlorate, Na chlorate, and Na perchlorate chlorinated and oxidized the most PAHs and their thermal decomposition products (Fig. 4 and Table 2). Regardless of the nature of the PAH, Ca perchlorate had a minor influence whereas Mg perchlorate and K chlorate reacted with more than half of the pyrolyzates. The chlorination and oxidation of aromatic rings are referenced in the literature and can explain most of the chemical reactions observed in our analyses [64]. In short, the (oxy)chlorinated and oxidized compounds detected are products from chemical reactions between PAHs and their pyrolyzates and the gases released during the thermal decomposition of the salts (O_2 and HCl/Cl_2). These chemical reactions usually require high temperatures which were reached during flash-pyrolysis experiments. For example, the chloronaphthalene isomers were formed by direct monochloration of the naphthalenic core by chlorine. The decreasing abundance of the methylnaphthalene isomers

in presence of salts suggest a second hypothesis; chlorine may have substituted the alkyl group from methylnaphthalene to form both chloronaphthalene isomers. The formation of the di- and trichloronaphthalene isomers also suggest the substitution of hydrogen atoms from the PAHs by chlorine. In addition, the detection of numerous hydrogenated compounds indicates that they can be formed through hydrogenation by the water released from the silica and/or the salts. The increasing number of hydrogenated compounds after pyrolysis in the presence of salts indicate that they can also be formed from the hydrogen atoms that the chlorine atoms substituted for during the reactions.

Our results indicate that the three PAHs were thermally and chemically very stable as shown by their high resistance to high temperatures and salts. This is expected since the thermal and chemical stability of PAHs is directly related to the stability of the π-system of the molecule known to increase with its aromaticity [65]. This trend is observed in our results with an overall decrease in the number of thermal decomposition products in phenanthrene and benzanthracene compared to naphthalene when they are mixed in silica. In the presence of salts, the trend is similar with a general decrease in the number of pyrolyzates (Fig. 4). Except some minor variations due to the type of salt, the PAHs had a similar behavior regarding (oxy)chlorination and oxidation and the salts have not reacted with most of the PAHs and their pyrolyzates released during their thermal decomposition to form the new compounds detected. Benzanthracene was the least stable specifically in the presence of Na chlorate. Based on these results, the oxychlorine phases targeted can be placed in three categories which are consistent with their decomposition temperatures:

1. **Fe perchlorate and Na chlorate** (<400°C) had the highest oxidation and (oxy)chlorination power and reacted mostly with the parent PAH. This is confirmed by the relative abundances of certain pyrolyzates which remained within the same order of magnitude with these salts;
2. **Ca and Na perchlorates** (> 500°C) had a minor influence on the PAHs and their pyrolyzates and did not "transform" nor degrade them significantly;
3. **Mg perchlorate and K chlorate** (~500°C) were the most destructive and degraded and/or strongly reacted with both the parent molecule and pyrolyzates likely through combustion by O_2. Compounds were most likely released into CO_2 or into other light molecules that cannot be retrieved or deconvolved in our analytical conditions. These results are consistent with studies which showed that when pyrolyzed with Mg perchlorate, the concentration of organics should be at least five times higher than Mg perchlorate for the organics to be detected, enhancing their highly destructive power compared to the other salts [41].

Several hypotheses can explain the distinct behavior of Fe perchlorate compared to the other salts:

(1) Its final residue after heating is FeO [43,44], meaning that HCl and Cl_2 are entirely released and able to react with the parent molecules and its pyrolyzates. The EGA of Fe perchlorate (Fig. 1) shows two HCl and Cl_2 releases, lending credibility to this hypothesis. However, as a metallic perchlorate, the residue of Mg perchlorate is MgO as well, and despite the similar HCl and Cl_2 releases observed in EGA, it did not chlorinate or oxidize PAHs as much as Fe perchlorate.

(2) The Fe perchlorate selected for this study was hydrated. The EGA of Fe perchlorate indicated three H_2O steps release, two of which corresponded to its dehydration steps. The H_2O released would thus react with Cl_2 to form HCl in higher amount compared to the other salts which would easily further react with the PAHs and their pyrolyzates. This hypothesis seems also unlikely because a similar EGA was obtained for Mg perchlorate and it had a very different behavior compared to Fe perchlorate.

(3) Fe perchlorate decomposes at much lower temperature (~230°C) compared to the other salts. Despite the flash-pyrolysis that was used, the species were released before or during the sublimation of the PAHs (~218°C for naphthalene, ~332°C for phenanthrene, ~438°C for benzanthracene) and were readily available to react with them and a portion of their pyrolyzates (Fig. 6). This hypothesis is the most likely since Na chlorate is in second position in terms of (oxy)chlorination and oxidation power and decomposes at low temperature right after Fe perchlorate at ~380°C, whereas all the other salts decompose at temperatures above 400°C.

3.5. *Influence of the concentration of Ca and Fe perchlorates on Naphthalene*

As shown above, PAHs were stable when pyrolyzed with two times more perchlorates and Fe perchlorate had the highest (oxy)chlorination power of all salts. But what happens if we increase the concentration of two selected perchlorates up to ten times more perchlorates compared to the amount of PAHs? Fig. 7 shows the comparative chromatograms obtained after the pyrolysis of naphthalene in the presence of Ca and Fe perchlorates at 1 and 5 wt% in silica.

Naphthalene was still detected despite the highest concentration of perchlorates but its relative abundance decreased by a factor 8 and 4 with 5 wt% of Ca and Fe perchlorates, respectively. This decrease was negligible when naphthalene was pyrolyzed with 1 wt% of perchlorate compared to no salt, indicating an impact of the increase concentration of perchlorate. This phenomenon can be explained by the reaction of a portion of naphthalene (about 80 and 40 % for Ca and Fe perchlorates, respectively) with the perchlorates to form new compounds during pyrolysis. Overall, naphthalene remained chemically stable after pyrolysis and should be detectable if it was present in a sample containing ten times more perchlorate. Other similar studies have shown that there should at least be five times more organics compared to perchlorates in the martian regolith to be detectable using pyrolysis [41]. However, these studies differ by the nature of the organic matter and perchlorate used and the sample preparation method. In particular, Mg perchlorate was used which, as shown here, is highly destructive to the organics compared to Ca and Fe perchlorates.

The total number of pyrolyzates (~71 and ~127 with Ca and Fe perchlorates at 1 wt%, respectively) decreased by 30 and 40 % at 5 wt%. With Fe perchlorate, the number of oxidized and (oxy)chlorinated compounds also decreased to ~14 and ~18. With Ca perchlorate, the number of oxidized compounds decreased by 50 % but the number of chlorinated compounds doubled. To have a better understanding of the influence of perchlorates on naphthalene's pyrolyzates, the relative abundances of benzene and indene were measured. With ten times more Ca and Fe perchlorate, the abundance of benzene remained similar

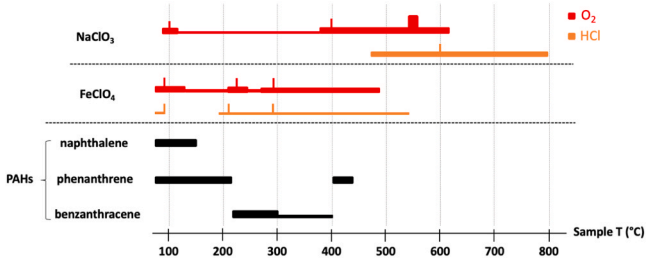

Fig. 6. Summary of the release temperatures of the volatiles O_2 and HCl for $NaClO_3$ and $FeClO_4$ which were the most impactful oxychlorines of all the salts targeted compared to the release temperatures of the three PAHs selected for this study. The release temperatures of all volatiles for all six salts can be found in the supplemental Fig. S1.

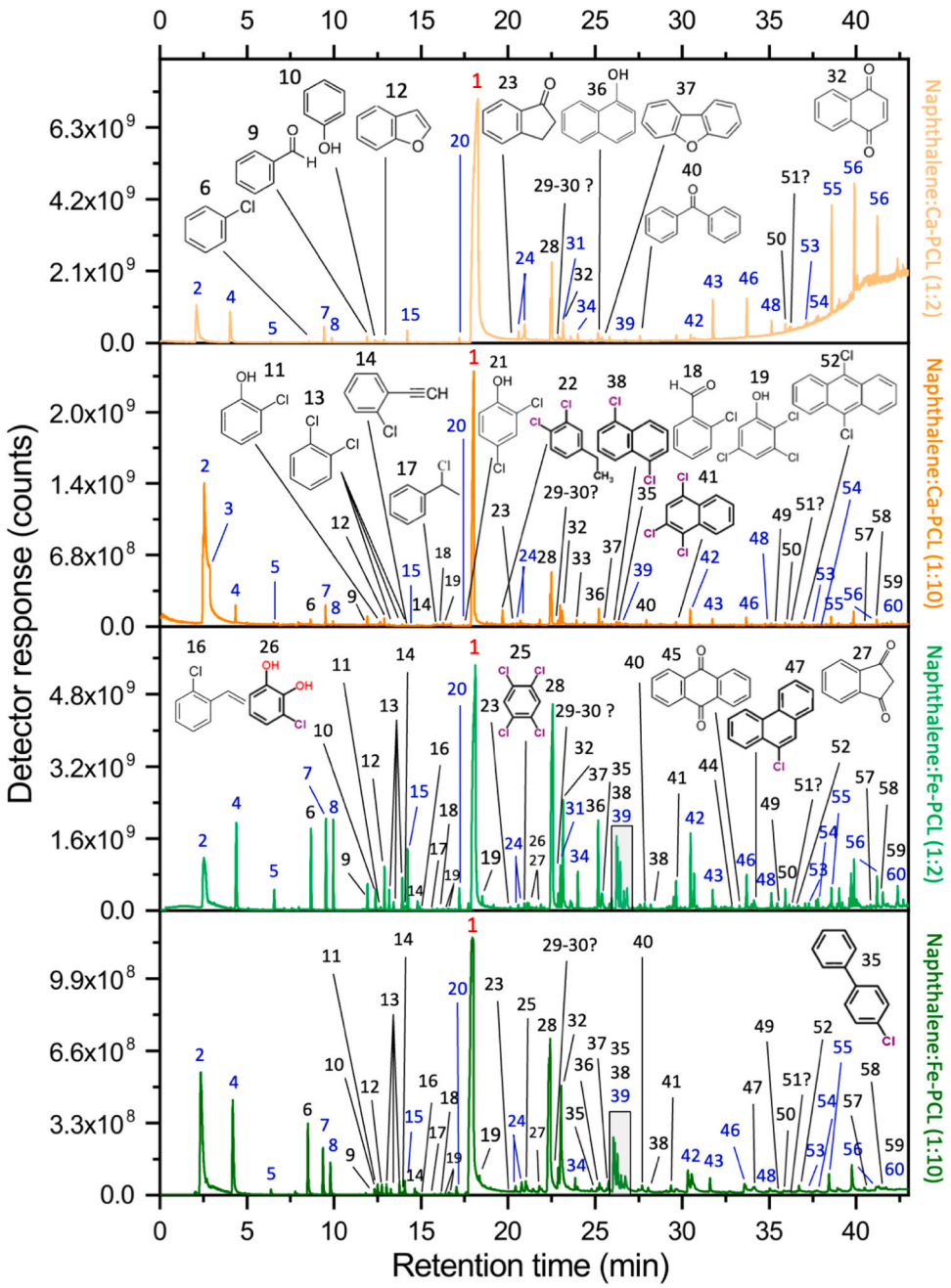

Fig. 7. Chromatograms obtained after the pyrolysis of naphthalene mixed with the Ca (Ca-PCL) and Fe (Fe-PCL) perchlorates in orange and green respectively, and mixed in 1 and 5 wt% in fused silica (light and dark color, respectively). To differentiate the pyrolyzates produced from the thermal decomposition of naphthalene to those produced from reactions with perchlorates, the former compounds were represented in blue and the latter in black. The structures of the molecules have been represented on the chromatograms where they appear for the first time. Compounds: 1: naphthalene, 2: CO_2, 3: HCl, 4: benzene, 5: toluene, 6: chlorobenzene, 7: phenylethyne, 8: styrene, 9: benzaldehyde, 10: phenol, 11:chlorophenol, 12: benzofuran, 13: 3x dichlorobenzene isomers, 14: chloroethynylbenzene, 15: indene, 16: chlorostyrene isomers, 17: chlorophenylethene, 18: chlorobenzaldehyde, 19: trichlorobenzene isomers, 20: methylindene, 21: dichlorophenol, 22: dichloroethylbenzene, 23: indanone, 24: methylnaphtalène isomers, 25: pentachlorobenzene, 26: chlorobenzenediol, 27: indandione, 28: chloronapthalene isomers, 29: hydroxy-cinnamic acid, 30: phenylpropenoyl chloride, 31: biphenylene, 32: naphtoquinone, 33: dichloroindane, 34: acenaphtylene, 35: chlorobiphenyle, 36: naphthalenol, 37: dibenzofuran, 38: dichloronaphthalene isomers, 39: fluorene, 40: benzophenone, 41: trichloronaphthalene isomers, 42: phenanthrene and anthracene, 43: vinylanthracene (or ethenylanthracene), 44: hydroxyfluorenone, 45: anthraquinone, 46: phenylnaphthalene isomers, 47: chlorophenanthrene isomers, 48: fluoranthene isomers, 49: chlorovinylanthracene, 50: indenochromene, 51: pyrenol or benzonaphtofurane (both in Fe-PCL), 52: dichlorophenantrene (or dichloroanthracene), 53: methylfluoranthene or isomer, 54: benzanthracene or isomer, 55: dihydrobenzopyrene, 56: 2x binaphthalene isomers, 57: chlorophenylmethylenefluorene, 58: dinaphtofuran, 59: naphthacenedione or isomer, and 60: dibenzofluorene.

compared to naphthalene in silica. The indene peak area decreased by an order of magnitude in 5 wt% Ca perchlorate but remained similar in either 1 or 5 wt% of Fe perchlorate. These results confirm that part of the gases released from the thermal decomposition of naphthalene reacted with Ca perchlorate to form the (oxy)chlorinated compounds detected, on the contrary to Fe perchlorate. The decrease in abundances in addition to the non-detection of certain compounds when the concentration of perchlorate was higher (e.g., phenol, biphenylene) confirm this hypothesis.

At 1 wt% Ca perchlorate, 86 % of the total number of pyrolyzates

were detected, compared to 61 % at 5 wt%. With 1 wt% Fe perchlorate, the number of pyrolyzates increased up to 141 %, indicating the production of new species resulting from its strong oxidation and (oxy) chlorination influence. The results obtained with 5 wt% Fe perchlorate were equivalent to the results with 1 wt% Ca perchlorate concentration. In addition, the abundances of the main compounds were relatively similar compared to naphthalene in silica. The fact that numerous naphthalene's pyrolyzates (i.e., not oxidized nor (oxy)chlorinated) were still present and in similar abundances with Fe perchlorate indicate that it only required a low amount of gases to form new compounds or that it reacted with the least stable thus confirming its high reactivity rate. Ca perchlorate reacted with more pyrolyzates to form the oxidized and (oxy)chlorinated compounds as shown by the general decrease in the number of pyrolyzates.

At a 1 wt% concentration, Fe perchlorate was more oxidizing and chlorinating than Ca perchlorate at the same concentration. With 5 wt% Ca perchlorate, its chlorination power increased over oxidation as shown by the formation of new (oxy)chlorinated compounds that were already formed with 1 wt% Fe perchlorate (e.g., chlorobenzaldehyde, trichlorobenzene isomers, di- and trichloronaphthalene isomers) but in lower concentration. For example, the relative abundance of chlorobenzene increased by 1.3 with 5 wt% of Ca perchlorate but was still smaller compared to 1 wt% of Fe perchlorate whereas it was equivalent with 5 wt% of Fe or Ca perchlorate.

After pyrolysis with Fe perchlorate regardless of concentration, new oxidized and (oxy)chlorinated compounds were produced: chlorostyrene isomers, chlorobenzenediol, tetrachlorobenzene, anthraquinone, chlorophenanthrene (or chloroanthracene), indandione, and chlorobiphenyl isomers. These compounds were not detected despite the increase in the concentration of Ca perchlorate. Chlorobenzenediol and chlorostyrene were formed exclusively at 5 wt% Fe perchlorate. Some chlorinated compounds were formed exclusively with 5 wt% of Ca perchlorate—dichloroethylbenzene, dichlorophenol, and dichloroindane. Even if a quantitative effect exists, the (oxy)chlorination power of Ca perchlorate never reached the (oxy)chlorination power of Fe perchlorate, as indicated by the production of certain chlorohydrocarbons exclusively with Fe perchlorate, and the relative abundances of the pyrolyzates.

Results showed that the nature of the cation plays an important role not only in the chlorination processes but also in the degradation of the organics as proven when confronted to similar studies [41]. We also confirmed the distinct behavior of Fe perchlorate compared to the other salts even with an increase in concentration which is likely due to its low decomposition temperature (~230°C) compared to the other salts which mostly decompose above 400°C.

4. Implications for the detection of PAHs on Mars

Results indicate that PAHs were not entirely thermally nor chemically degraded under the influence of the salts targeted in this study and even remained the major organic molecules detected. PAHs should thus be detectable in a martian sample despite the presence of oxychlorine salts. The variations in the stability of the molecule depend on the type of salt that was pyrolyzed with the PAHs and their physico-chemistry properties (size, structure, sterically hindered, boiling temperature). In addition, the nature of the perchlorate's cation is of major importance to interpret the results on organic detections on Mars. For example, Na chlorate degraded entirely benzanthracene. This could be due to the sublimation temperature of benzanthracene (~438°C) at the same time as the release of O_2 by Na chlorate (between 390 and 600°C), thus leading to its entire combustion into CO_2 and in the oxidized and chlorinated compounds detected. Other studies have also shown that aromatic hydrocarbons may be totally combusted in the presence of Mg perchlorates in lower concentrations compared to those used in this study [41]. Other factors may be at play such as the sample preparation method and the presence of minerals other than perchlorates which can either catalyze the destruction of organics or on the contrary have a protective effect [41,56–60].

If naphthalene was present in a martian sample, it should not react with perchlorate even in a sample containing ten times more Ca or Fe perchlorates. Naphthalene was indeed chemically stable and only slightly affected by the oxidizing conditions of the martian subsurface simulated by synthetic analogs, even during its thermal extraction at high temperature (~850°C). In addition, the compounds produced from reactions between the PAH pyzolyzates and the inorganic species released by the salts (O_2, HCl) could further help to identify the parent molecule present in a sample through the number of rings of the pyrolyzates. Typically, the presence of naphtoquinone and chloronaphthalene isomers, phenalenone, and chloroanthracene / chlorophenanthrene, and naphthacenequinone in the chromatograms of naphthalene, phenanthrene, and benzanthracene, respectively, are characteristic of the size and number of rings of the parent PAH pyrolyzed.

Our results show that if present on Mars, PAHs should be present in the flight chromatogram and detected alongside other molecules (e.g., chloronaphthalene). Despite the high abundance of PAHs in CC and micrometeorites regularly reaching the surface [30,37,66], the presence of indigenous PAHs nor chlorinated/oxidized PAHs on Mars has yet to be established. Indeed, PAHs (Naphthalene and derivatives-methyl-naphthalene and dihydronaphthalene) have only been tentatively identified by the SAM instrument and their origin(s) remain unclear [14]. However, the presence of kerogen-like material has been strongly suggested from the results obtained with the SAM instrument onboard the *Curiosity* rover, and the preliminary results obtained by the SHERLOC instrument suite onboard *Perseverance* seem to indicate the presence of aromatic compounds up to two rings [14,16,17]. The non-detection of PAHs larger than naphthalene and chlorine-bearing PAHs may be explained by technical constraints of the SAM instrument. Previous studies have shown that the retention time of some compounds is too long to be detectable within the current SAM analytical GC conditions [67,68]. Phenanthrene and benzanthracene have retention times beyond the maximum time of analysis of SAM (~21 min for the shortest time of analysis) regardless of the column used. The retention time of chloronaphthalene was measured as between 22.8 and 35 min and thus within the current SAM-flight conditions, may have been easily missed if not analyzed with the right column. This same study showed that other flight instrumental constraints could also play a role in the non-detection of PAHs. Specifically, the hydrocarbon and injection trap(s) used to pre-concentrate the volatiles prior to their desorption and introduction into the GC column could permanently retained PAHs [68].

The qualitative effect observed for compounds produced exclusively in the presence of a specific perchlorate regardless of their concentration (e.g., dichloroindane and dichloroethylbenzene produced exclusively with Ca perchlorate) highlight the fact that the cation plays a role in the chemical processes occurring during pyrolysis. Although these specific chemical processes remain unknown, the detection of compounds specific to a perchlorate could give clues on the nature of the salts present in a martian sample analyzed with pyr-GC/MS.

5. Precursors of the chlorohydrocarbons detected on Mars

Our results demonstrate the detection of numerous chlorohydrocarbons, mostly aromatics as expected from chemical reactions between the PAHs and the chlorinated species released by (per)chlorate salts. Chlorobenzene and dichlorobenzene isomers are the only compounds that were detected both on Mars with the SAM instrument [9,10] and in our laboratory experiments. Although our results indicate that PAHs are possible candidate of the precursors of the martian aromatic chlorohydrocarbons, they should have been detected alongside other molecules on Mars such as the parent molecule itself and characteristic chlorinated molecule (e.g., chloronaphthalene) regardless of the type of

pyrolysis [12]. As long as the technical constraints of SAM are not proven to be a limiting parameter in detecting PAHs, it is likely that the martian aromatic chlorohydrocarbons were produced from reactions between salts and organic chemical families other than PAHs. So far, benzoic acid has been suggested as one of the most likely candidate precursors of the chlorobenzene detected on Mars [69] and its recent detection on Mars [70], in tandem with the results presented in this study, lend support to this hypothesis.

6. Conclusion

This study showed that the PAHs–naphthalene, phenanthrene, and benzanthracene–as well as their pyrolyzates were not significantly degraded by salts with the exception of benzanthracene with Na chlorate. PAHs have similar behaviors regarding the oxidation and (oxy) chlorination by salts: Fe perchlorate had the strongest influence followed in decreasing order by Na chlorate, Na perchlorate, and Ca perchlorate, and Mg perchlorate and K chlorate which were the most destructive. We showed that Fe perchlorate has the highest chlorination power and may catalyze thermal decomposition of the molecules, a high reactivity rate that could be explained by three hypothesis: (1) its degree of hydration, (2) its final residue after heating, which is iron oxide (FeO), or more likely (3) its lowest degradation temperature (~230°C) compared to the other salts.

Several parameters may influence the degradation and (oxy)chlorination processes of PAHs. The nature of the molecule itself, its size, and number of rings, play a role in not only the thermal but also in the chemical stability of the PAH. The different behaviors observed regarding salts can be explained by the sublimation temperatures of the PAHs and the release temperatures of the salts which can favor oxidation over chlorination processes or vice versa. This was, for example, observed with benzanthracene, which seemed more affected by oxidation as opposed to chlorination. The processes of oxidation by O_2 and chlorination by HCl and/or Cl_2 are competing, and depending on the nature of the salt and the parent molecule, one process over the other will likely be favored, even when using fast flash-pyrolysis ramp.

This study also highlights the chlorination processes involved during the pyrolysis of PAHs with salts, which depend on both the type of salt and the parent molecule. For example, the interaction of naphthalene with Fe perchlorate produced a family of unsaturated aliphatic chlorohydrocarbons typical of the interaction between this PAH/salt couple: the di-, tri- and tetrachloroethene isomer. In addition, the pyrolyzates produced through oxidation and/or (oxy)chlorination processes can reflect the parent PAH pyrolyzed (e.g., chloronaphthalene), compounds that could be used to identify the PAH originally present in martian sample before thermal extraction even in relatively high concentration.

This work shows that PAHs can be the precursors of the aromatic chlorohydrocarbons detected on Mars. However, the non-detection of the parent PAH itself and of its chlorinated derivatives up today with the SAM instrument tend to discredit this hypothesis, unless the analytical conditions used in flight are proven to be the limiting factor for their detection. Answers may soon be obtained by the analysis of future samples with the SAM instrument and in the mid-term with the future MOMA (Mars Organic Molecule Analyser) instrument. Onboard the *Rosalind Franklin* rover scheduled to land in 2028 at *Oxia Planum*, the MOMA instrument will be able to analyze samples that will be collected deeply into the subsurface (down to two meters) and to reach organic molecules that have been protected from the harsh conditions of the martian surface. In addition, the NASA/ESA joined Mars Sample Return (MSR) campaign as well as the JAXA MMX mission will return samples from Mars and its satellite Phobos in 2033 and 2029, respectively, which should clarify the origin(s), distribution, and abundance of PAHs in martian near-surface materials.

Declaration of Competing Interest

The authors declare that they have no known competing financial interests or personal relationships that could have appeared to influence the work reported in this paper.

Data Availability

Data will be made available on request.

Acknowledgements

This work was supported by CNES, focused on Sample Analysis at Mars and on Mars Science Laboratory. M.M. and S.S.J. acknowledge the funding from the NASA-GSFC grant NNX17AJ68G: “Using Organic Molecule Detections in Mars Analog Environments to Interpret the Results of the SAM Investigation on the MSL Mission.”

Author agreement statement

We the undersigned declare that this manuscript is original, has not been published before and is not currently being considered for publication elsewhere. We confirm that the manuscript has been read and approved by all named authors and that there are no other persons who satisfied the criteria for authorship but are not listed. We further confirm that the order of authors listed in the manuscript has been approved by all of us. We understand that the Corresponding Author is the sole contact for the Editorial process. He/she is responsible for communicating with the other authors about progress, submissions of revisions and final approval of proofs

Appendix A. Supporting information

Supplementary data associated with this article can be found in the online version at doi:10.1016/j.jaap.2024.106578.

References

[1] K. Biemann, J. Oro, P. Toulmin, L.E. Orgel, A.O. Nier, D.M. Anderson, P. G. Simmonds, D. Flory, A.V. Diaz, D.R. Rushneck, J.E. Biller, L. Lafleur, J. Geophys. Res. 82 (1977) 4641.
[2] K. Biemann, J. Oro, P. Toulmin, L.E. Orgel, A.O. Nier, D.M. Anderson, P. G. Simmonds, D. Flory, A.V. Diaz, D.R. Rushneck, J.A. Biller, Science 194 (1976) 72.
[3] M.H. Hecht, S.P. Kounaves, R.C. Quinn, S.J. West, S.M.M. Young, D.W. Ming, D. C. Catling, B.C. Clark, W.V. Boynton, J. Hoffman, L.P. DeFlores, K. Gospodinova, J. Kapit, P.H. Smith, Science 325 (2009) 64.
[4] B. Sutter, R. Quinn, P. Archer, D. Glavin, T. Glotch, S. Kounaves, M. Osterloo, E. Rampe and D. Ming, (2016).
[5] D.P. Glavin, C. Freissinet, K.E. Miller, J.L. Eigenbrode, A.E. Brunner, A. Buch, B. Sutter, P.D. Archer, S.K. Atreya, W.B. Brinckerhoff, M. Cabane, P. Coll, P. G. Conrad, D. Coscia, J.P. Dworkin, H.B. Franz, J.P. Grotzinger, L.A. Leshin, M. G. Martin, C. McKay, D.W. Ming, R. Navarro-González, A. Pavlov, A. Steele, R. E. Summons, C. Szopa, S. Teinturier, P.R. Mahaffy, J. Geophys. Res.: Planets 118 (2013) 1.
[6] R. Navarro-Gonzalez, E. Vargas, J. de la Rosa, A.C. Raga, C.P. McKay, J. Geophys. Res. -Planets 115 (2010).
[7] M. Guzman, C.P. McKay, R.C. Quinn, C. Szopa, A.F. Davila, R. Navarro-González, C. Freissinet, J. Geophys. Res.: Planets 123 (2018) 1674.
[8] J. Lewis, J. Eigenbrode, G. Wong, A. McAdam, P. Archer, B. Sutter, M. Millan, R. Williams, M. Guzman, A. Das, J. Geophys. Res.: Planets 126 (2021) e2020JE006803.
[9] C. Szopa, C. Freissinet, D.P. Glavin, M. Millan, A. Buch, H.B. Franz, R.E. Summons, D.Y. Sumner, B. Sutter, J.L. Eigenbrode, Astrobiology 20 (2020) 292.
[10] C. Freissinet, D.P. Glavin, P.R. Mahaffy, K.E. Miller, J.L. Eigenbrode, R. E. Summons, A.E. Brunner, A. Buch, C. Szopa, P.D. Archer, H.B. Franz, S.K. Atreya, W.B. Brinckerhoff, M. Cabane, P. Coll, P.G. Conrad, D.J. Des Marais, J.P. Dworkin, A.G. Fairen, P. Francois, J.P. Grotzinger, S. Kashyap, I.L. ten Kate, L.A. Leshin, C. A. Malespin, M.G. Martin, F.J. Martin-Torres, A.C. McAdam, D.W. Ming, R. Navarro-Gonzalez, A.A. Pavlov, B.D. Prats, S.W. Squyres, A. Steele, J.C. Stern, D. Y. Sumner, B. Sutter, M.P. Zorzano, M.S.L.S. Team, J. Geophys. Res. -Planets 120 (2015) 495.

[11] A. Buch, C. Szopa, C. Freissinet, D. Boulesteix, F. Stalport, S. Nowak, N. Chaouche, P. Gilbert and D. Coscia, *Influence of the secondary X-Rays on the organic matter at Mars' near-surface*, at: AGU Fall Meeting Abstracts, P12A.

[12] M. Millan, C. Szopa, A. Buch, R. Summons, R. Navarro-Gonzalez, P. Mahaffy, S. Johnson, J. Geophys. Res.: Planets 125 (2020) e2019JE006359.

[13] J. Clark, B. Sutter, P.D. Archer Jr, D. Ming, E. Rampe, A. McAdam, R. Navarro-González, J. Eigenbrode, D. Glavin, M.-P. Zorzano, Minerals 11 (2021) 475.

[14] M. Millan, A.J. Williams, A.C. Mcadam, J.L. Eigenbrode, A. Steele, C. Freissinet, D. P. Glavin, C. Szopa, A. Buch, R.E. Summons, J. Geophys. Res.: Planets 127 (2022) e2021JE007107.

[15] A.H. Ansari, Front. Astron. Space Sci. 10 (2023) 1075052.

[16] J.L. Eigenbrode, R.E. Summons, A. Steele, C. Freissinet, M. Millan, R. Navarro-González, B. Sutter, A.C. McAdam, H.B. Franz, D.P. Glavin, Science 360 (2018) 1096.

[17] S. Sharma, R.D. Roppel, A.E. Murphy, L.W. Beegle, R. Bhartia, A. Steele, J.R. Hollis, S. Siljeström, F.M. McCubbin, S.A. Asher, Nature (2023) 1.

[18] B. Sutter, A.C. McAdam, P.R. Mahaffy, D.W. Ming, K.S. Edgett, E.B. Rampe, J. L. Eigenbrode, H.B. Franz, C. Freissinet, J.P. Grotzinger, A. Steele, C.H. House, P. D. Archer, C.A. Malespin, R. Navarro-González, J.C. Stern, J.F. Bell, F.J. Calef, R. Gellert, D.P. Glavin, L.M. Thompson, A.S. Yen, J. Geophys. Res.: Planets 122 (2017) 2574.

[19] J. Clark, B. Sutter, R. Morris, P. Archer, D. Ming, P. Niles, P. Mahaffy and R. Navarro-Gonzalez, (2016).

[20] L. Ojha, M.B. Wilhelm, S.L. Murchie, A.S. McEwen, J.J. Wray, J. Hanley, M. Masse, M. Chojnacki, Nat. Geosci. 8 (2015) 829.

[21] P.D. Archer, H.B. Franz, B. Sutter, R.D. Arevalo, P. Coll, J.L. Eigenbrode, D. P. Glavin, J.J. Jones, L.A. Leshin, P.R. Mahaffy, A.C. McAdam, C.P. McKay, D. W. Ming, R.V. Morris, R. Navarro-Gonzalez, P.B. Niles, A. Pavlov, S.W. Squyres, J. C. Stern, A. Steele, J.J. Wray, J. Geophys. Res. -Planets 119 (2014) 237.

[22] L.A. Leshin, P.R. Mahaffy, C.R. Webster, M. Cabane, P. Coll, P.G. Conrad, P. D. Archer, S.K. Atreya, A.E. Brunner, A. Buch, J.L. Eigenbrode, G.J. Flesch, H. B. Franz, C. Freissinet, D.P. Glavin, A.C. McAdam, K.E. Miller, D.W. Ming, R. V. Morris, R. Navarro-Gonzalez, P.B. Niles, T. Owen, R.O. Pepin, S. Squyres, A. Steele, J.C. Stern, R.E. Summons, D.Y. Sumner, B. Sutter, C. Szopa, S. Teinturier, M.G. Trainer, J.J. Wray, J.P. Grotzinger, Science 341 (2013) 9.

[23] D.W. Ming, P.D. Archer, D.P. Glavin, J.L. Eigenbrode, H.B. Franz, B. Sutter, A. E. Brunner, J.C. Stern, C. Freissinet, A.C. McAdam, P.R. Mahaffy, M. Cabane, P. Coll, J.L. Campbell, S.K. Atreya, P.B. Niles, J.F. Bell, D.L. Bish, W. B. Brinckerhoff, A. Buch, P.G. Conrad, D.J. Des Marais, B.L. Ehlmann, A.G. Fairen, K. Farley, G.J. Flesch, P. Francois, R. Gellert, J.A. Grant, J.P. Grotzinger, S. Gupta, K.E. Herkenhoff, J.A. Hurowitz, L.A. Leshin, K.W. Lewis, S.M. McLennan, K. E. Miller, J. Moersch, R.V. Morris, R. Navarro-Gonzalez, A.A. Pavlov, G.M. Perrett, I. Pradler, S.W. Squyres, R.E. Summons, A. Steele, E.M. Stolper, D.Y. Sumner, C. Szopa, S. Teinturier, M.G. Trainer, A.H. Treiman, D.T. Vaniman, A.R. Vasavada, C.R. Webster, J.J. Wray, R.A. Yingst, M.S.L.S. Team, Science 343 (2014).

[24] S.P. Kounaves, B.L. Carrier, G.D. O'Neil, S.T. Stroble, M.W. Claire, Icarus 229 (2014) 206.

[25] B. Sutter, D. Archer, D. Ming, P. Niles, J. Eigenbrode, H. Franz, D. Glavin, A. McAdam, P. Mahaffy and J. Stern, (2014).

[26] P. Archer, D. Ming, B. Sutter, R. Morris, B. Clark, P. Mahaffy, J. Wray, A. Fairen, R. Gellert and A. Yen, *Oxychlorine Species on Mars: Implications from Gale Crater Samples*, at: Lunar and Planetary Science Conference, 2947.

[27] F. Salama, Proc. Int. Astron. Union 4 (2008) 357.

[28] B.P. Basile, B.S. Middleditch, J. Oró, Org. Geochem. 5 (1984) 211.

[29] H. Naraoka, A. Shimoyama, M. Komiya, H. Yamamoto, K. Harada, Chem. Lett. 17 (1988) 831.

[30] M.A. Sephton, Nat. Prod. Rep. 19 (2002) 292.

[31] O. Botta, J.L. Bada, Surv. Geophys. 23 (2002) 411.

[32] M. Sephton, G. Love, J. Watson, A. Verchovsky, I. Wright, C. Snape, I. Gilmour, Geochim. Et. Cosmochim. Acta 68 (2004) 1385.

[33] S. Pizzarello, G.W. Cooper, G.J. Flynn, H.Y. McSween, D.S. Lauretta, Meteor. Early Sol. Syst. II (2006) 625 (Ed.).

[34] D.P. Glavin, C.M.D. Alexander, J.C. Aponte, J.P. Dworkin, J.E. Elsila, H. Yabuta, in *Primitive meteorites and asteroids*, Elsevier, 2018, p. 205.

[35] M. Zolotov, E. Shock, J. Geophys. Res. -Planets 104 (1999) 14033.

[36] A. Steele, F.M. McCubbin, M. Fries, L. Kater, N.Z. Boctor, M.L. Fogel, P.G. Conrad, M. Glamoclija, M. Spencer, A.L. Morrow, M.R. Hammond, R.N. Zare, E.P. Vicenzi, S. Siljestrom, R. Bowden, C.D.K. Herd, B.O. Mysen, S.B. Shirey, H.E.F. Amundsen, A.H. Treiman, E.S. Bullock, A.J.T. Jull, Science 337 (2012) 212.

[37] S.J. Clemett, X.D.F. Chillier, S. Gillette, R.N. Zare, M. Maurette, C. Engrand, G. Kurat, Orig. Life Evol. Biospheres 28 (1998) 425.

[38] R.V. Morris, D.T. Vaniman, D.F. Blake, R. Gellert, S.J. Chipera, E.B. Rampe, D. W. Ming, S.M. Morrison, R.T. Downs, A.H. Treiman, A.S. Yen, J.P. Grotzinger, C. N. Achilles, T.F. Bristow, J.A. Crisp, D.J. Des Marais, J.D. Farmer, K.V. Fendrich, J. Frydenvang, T.G. Graff, J.M. Morookian, E.M. Stolper, S.P. Schwenzer, Proc. Natl. Acad. Sci. USA 113 (2016) 7071.

[39] S.W. Squyres, R.E. Arvidson, S. Ruff, R. Gellert, R.V. Morris, D.W. Ming, L. Crumpler, J.D. Farmer, D.J.Des Marais, A. Yen, S.M. McLennan, W. Calvin, J. F. Bell, B.C. Clark, A. Wang, T.J. McCoy, M.E. Schmidt, P.A. de Souza, Science 320 (2008) 1063.

[40] H.R. Schulten, P. Leinweber, Plant Soil 151 (1993) 77.

[41] S.H. Royle, E. Oberlin, J.S. Watson, W. Montgomery, S.P. Kounaves, M.A. Sephton, J. Geophys. Res.: Planets 123 (2018) 1901.

[42] K.M. Cannon, B. Sutter, D.W. Ming, W.V. Boynton, R. Quinn, Geophys. Res. Lett. 39 (2012).

[43] M.M. Markowitz, J. Inorg. Nucl. Chem. 25 (1963) 407.

[44] G.G. Marvin, L.B. Woolaver, Ind. Eng. Chem. Anal. Ed. 17 (1945) 474.

[45] A. Migdał-Mikuli, J. Hetmańczyk, J. Therm. Anal. Calorim. 91 (2008) 529.

[46] X.F. Dong, Q.L. Yan, X.H. Zhang, D.L. Cao, C.L. Xuan, J. Anal. Appl. Pyrolysis 93 (2012) 160.

[47] T. Wydeven, J. Catal. 19 (1970) 162.

[48] O. McIntosh, C. Freissinet, A. Buch, J. Lewis, M. Millan, A. Williams, T. Fornaro, J. Eigenbrode, J. Brucato, C. Szopa, Icarus (2024) 116015.

[49] S.W. Ruff, J.D. Farmer, Nat. Commun. 7 (1) (2016).

[50] J. Tarnas, J. Mustard, H. Lin, T. Goudge, E. Amador, M. Bramble, C. Kremer, X. Zhang, Y. Itoh, M. Parente, Geophys. Res. Lett. 46 (2019) 12771.

[51] M. Pineau, L. Le Deit, B. Chauviré, J. Carter, B. Rondeau, N. Mangold, Icarus 347 (2020) 113706.

[52] S.C. Moldoveanu, Pyrolysis of organic molecules: applications to health and environmental issues, Elsevier, 2009.

[53] K.A. Bennett, V.K. Fox, A. Bryk, W. Dietrich, C. Fedo, L. Edgar, M.T. Thorpe, A. J. Williams, G.M. Wong, E. Dehouck, J. Geophys. Res.: Planets 128 (2023) e2022JE007185.

[54] B.L. Ehlmann, C.S. Edwards, R. Jeanloz, Annu. Rev. Earth Planet. Sci. *Vol 42* (2014) 291 (Ed.).

[55] T. Bristow, J. Grotzinger, E. Rampe, J. Cuadros, S. Chipera, G. Downs, C. Fedo, J. Frydenvang, A. McAdam, R. Morris, Science 373 (2021) 198.

[56] P. Francois, C. Szopa, A. Buch, P. Coll, A.C. McAdam, P.R. Mahaffy, C. Freissinet, D. P. Glavin, R. Navarro-Gonzalez, M. Cabane, J. Geophys. Res. -Planets 121 (2016) 61.

[57] J.M.T. Lewis, J.S. Watson, J. Najorka, D. Luong, M.A. Sephton, Astrobiology 15 (2015) 247.

[58] S.H. Royle, T.L. Salter, J.S. Watson, M.A. Sephton, Astrobiology 22 (2022) 520.

[59] S.H. Royle, J.S. Tan, J.S. Watson, M.A. Sephton, Astrobiology 21 (2021) 673.

[60] T.L. Salter, J.S. Watson, M.A. Sephton, J. Anal. Appl. Pyrolysis 170 (2023) 105900.

[61] M.A. Sephton, J.S. Tan, J.S. Watson, K. Hickman-Lewis, J.M. Madariaga, J. Geol. Soc. 180 (2023) jgs2022.

[62] H. Steininger, F. Goesmann, W. Goetz, Planet. Space Sci. 71 (2012) 9.

[63] W. Montgomery, E.A. Jaramillo, S.H. Royle, S.P. Kounaves, D. Schulze-Makuch, M. A. Sephton, Astrobiology 19 (2019) 711.

[64] R. LOZE, Tech. De. l'Ing. énieur. Génie Des. Proc. éD. éS. 5 (1998). J5620. 1.

[65] J. Poater, M. Duran, M. Solà, Front. Chem. (2018) 561.

[66] G.J. Flynn, Earth Moon Planets 72 (1996) 469.

[67] M. Millan, C. Szopa, A. Buch, M. Cabane, S. Teinturier, P. Mahaffy, S.S. Johnson, J. Chromatogr. A 1598 (2019) 183.

[68] M. Millan, C. Szopa, A. Buch, P. Coll, D.P. Glavin, C. Freissinet, R. Navarro-Gonzalez, P. François, D. Coscia, J.Y. Bonnet, S. Teinturier, M. Cabane, P. R. Mahaffy, Planet. Space Sci. 129 (2016) 88.

[69] C. Freissinet, C.A. Knudson, H.V. Graham, J.M. Lewis, J. Lasue, A.C. McAdam, S. Teinturier, C. Szopa, E. Dehouck, R.V. Morris, Planet. Sci. J. 1 (2020) 41.

[70] M. Millan, S. Teinturier, C.A. Malespin, J.Y. Bonnet, A. Buch, J.P. Dworkin, J.L. Eigenbrode, C. Freissinet, D.P. Glavin, R. Navarro-González, A. Srivastava, J.C. Stern, B. Sutter, C. Szopa, A.J. Williams, R.H. Williams, G.M. Wong, S.S. Johnson and P.R. Mahaffy, *Nature Astronomy*, (2021).